NASA CR-151952

STANFORD UNIVERSITY

CENTER FOR SYSTEMS RESEARCH

FINAL REPORT

ON THE APPLICABILITY OF INTEGRATED CIRCUIT TECHNOLOGY TO GENERAL AVIATION ORIENTATION ESTIMATION

(NASA-CR-151952) ON THE APPLICABILITY OF INTEGRATED CIRCUIT TECHNOLOGY TO GENERAL AVIATION ORIENTATION ESTIMATION Final Report (Stanford Univ.) 78 p HC A05/MF A01 CSCL 09C G3/33

N77-17356

Unclas
14977

Guidance and Control Laboratory

submitted to

NASA AMES RESEARCH CENTER
Moffett Field, California 94035

Technical Monitor
Dr. Dallas Denery, MS: 210-9 FSN

Contract No. NAS-2-9083

Department of Aeronautics and Astronautics
Stanford, California 94305

Professor Daniel B. DeBra, Principal Investigator
Dr. Michael G. Fashler
with contributions from
Dr. John Sorensen, NRC Fellow

December 1976

Final Report

ON THE APPLICABILITY OF INTEGRATED CIRCUIT TECHNOLOGY TO GENERAL AVIATION ORIENTATION ESTIMATION

submitted to

NASA AMES RESEARCH CENTER
Moffett Field, California 94035

Technical Monitor
Dr. Dallas Denery, MS: 210-9 FSN

Contract No. NAS-2-9083

by

Stanford University
Guidance & Control Laboratory
Department Aeronautics and Astronautics
Stanford, California 94305

Principal Investigator
Professor Daniel B. DeBra

with contributions from
Dr. John Sorensen, NRC Fellow

September 1976

TABLE OF CONTENTS

Final Report

ON THE APPLICABILITY OF INTEGRATED CIRCUIT TECHNOLOGY TO GENERAL AVIATION ORIENTATION ESTIMATION

Chapter I

A. INTRODUCTION

1. Current Sensors for General Aviation

Many of the panel instruments used in general aviation have remained unchanged for over half a century. They work and pilots are familiar with their use. Considering the retraining required to familiarize nearly a million pilots with new displays, it is important that significant valve is established before a change is seriously considered. Criteria include ease of interpretation, reliability, weight, cost, power, and repairability.

2. Advances in Semiconductors/Sensors

The advances in analog and digital integrated circuits is well known. There has been a similar advance in sensor technology which has resulted in part from the technology developed to manufacture semiconductor devices. Pressure transducers and more recently, accelerometers, have been developed which are extremely small and low in cost. The continuation of this development is expected. Devices of this type make possible an integrated package of sensors which would change the single function sensor and display module format of the past and replace them with a single sensing package which could be used to drive a variety of displays and/or autopilot functions.

3. The Estimator

The other development which can change the approach to orientation sensing is in the field of information processing. Many times there is

coupling between states needed for display or control which can be modelled mathematically. Instead of requiring a measurement for every state, a few measurements used in conjunction with the appropriate models can be used to generate all the desired states. The formality of this process is extensively documented under the names of Kalman Filtering, Estimation Theory, or Observer Theory -- according to the nature of the problem. These theories make it possible to incorporate linear and angular accelerometers, magnetometers, and air data in an efficient way to estimate angular and linear velocities, heading and orientation states. Hence the information processing makes it possible to incorporate the new sensor technology and to avoid duplication in sensors to the greatest extent possible. It also provides a framework for comparing different models, e.g., kinematic equations vs dynamic equations, or a combination of some of each.

4. Scope of the Research

This research has examined some early discussion [Ref. 1] and added kinematic equations for comparison. An instrument survey has been performed to establish the present state of the art in linear and angular accelerometers, pressure transducers, and magnetometers. Gyros have not been included as they are reasonably well known and one goal of the research has been to establish if they could be omitted and still obtain an acceptable system. A very preliminary evaluation has been done of the computers available for data evaluation and estimator mechanization.

The report develops the theory used, documents the mathematical model of a light twin aircraft employed in the evaluation, presents the results of the sensor survey and discusses the results of the design studies.

In addition to personnel at Stanford: R.A. Van Patten, R. Clappier, Russ Hacker, and D. B. DeBra, a subcontract with Stanford Research Institute enabled us to benefit from the expert assistance of Dr. M. G. Tashker. Our work was coordinated through Dr. Denery at NASA Ames with similar work being done by Dr. J. A. Sorensen as an NRC Fellow. This report contains portions of Dr. Sorensen's work.

The work was closely integrated; the longitudinal equations and estimator represent Dr. Sorensen's work, though there are contributions throughout from all parties concerned.

II THEORY

A. GENERAL FORMULATION

For a general system written in state-variable notation

$$\dot{x} = Fx + Gu + \Gamma w \tag{2.1}$$

with control vector u and disturbance vector w and measurements

$$z = H_1 x + v \tag{2.2}$$

with measurement noise v, an estimator is formed as

$$\dot{\hat{x}} = F\hat{x} + Gu + K\,(z-\hat{z}) \tag{2.3}$$

For systems where measurements are made of the derivatives of the states, the measurement can be written

$$z = H_1 + H_2\dot{x} + v \tag{2.4}$$

If the derivative of the state is replaced by substitution from the state equation then

$$z = (H_1 + H_2F)x + H_2Gu + H_2\Gamma w + v \tag{2.5}$$

and the measurement equation contains noise that is correlated with the noise in the state equation. Since optimal control techniques require that the measurement and plant noise be uncorrelated, a new technique is required.

If $\overline{H}$ and $\overline{v}$ are defined as

$$\overline{H} = H_1 + H_2F \tag{2.6}$$

$$\bar{v} = H_2 \Gamma w + v \tag{2.7}$$

then the measurement may be written

$$z = \bar{H}x + H_2 G u + \bar{v} \tag{2.8}$$

and the state equation may have added to it a quantity that is identically equal to 0, multiplied by a constant L

$$\dot{x} = Fx + Gu + \Gamma w + L(z - \bar{H}x - H_2 G u - \bar{v}) \tag{2.9}$$

which, with the following definition

$$\bar{F} = F - L\bar{H} \tag{2.10}$$

$$\bar{G} = (I - LH_2)G \tag{2.11}$$

$$\bar{w} = \Gamma w - L\bar{v} \tag{2.12}$$

may be rewritten

$$\dot{x} = \bar{F}x + \bar{G}u + Lz + \bar{w} \tag{2.13}$$

If the covariance of the state noise w is Q, and that of the measurement noise v is R, then the covariances of the equivalent noises $\bar{w}$ and $\bar{v}$ are

$$\bar{Q} = E(\bar{w}\bar{w}^T) = (I - LH_2)\Gamma Q \Gamma^T (I - LH_2)^T + LRL^T \tag{2.14}$$

$$\bar{R} = E(\bar{v}\bar{v}^T) = R + H_2 \Gamma Q \Gamma^T H_2^T \tag{2.15}$$

and L may be chosen to decorrelate the equivalent state and measurement noise, $E(\bar{w}\bar{v}^T) = 0$,

$$L = \bar{R}^{-1} \Gamma Q \Gamma^T H_2^T \tag{2.16}$$

An estimator can be built for this system since Lz is known

$$\dot{\hat{x}} = \bar{F}\hat{x} + \bar{G}u + Lz + \bar{K}(z-\hat{z}) \qquad (2.17)$$

where

$$\hat{z} = H\hat{x} + \bar{H}_2 G\dot{u} \qquad (2.18)$$

This design can be performed by root square locus, eigenvalue decomposition, or pole placement techniques. After the value of $\bar{K}$ has been calculated using the equation above, the estimator can be mechanized by resubstituting the definition of $\bar{F}$ and $\bar{G}$ which yields

$$\dot{\hat{x}} = F\hat{x} + Gu + (L+\bar{K})(z-\hat{z}) \qquad (2.19)$$

where $\bar{K}$ has been found from the reformulated problem, and L is given in equation (2.16). Equation (2.19) is preferable to equation (2.17) because it is not driven by the measurement and because it will have the same behavior as the original plant, which is already familiar to the design engineer. The gain $(L + \bar{K})$ is the particular value of K which minimizes the expected error in the estimator with measurements of state derivatives.

If the system is designed by pole placement or other methods not associated with optimal control, the estimator is mechanized as in equation (2.19) with gain chosen to yield the desired performance. The following derivation of the estimator error equations holds regardless of the method used to determine the estimator gain. In this case, the estimator is mechanized with estimated values of the system matrix $\hat{F}$, and the control distribution matrix $\hat{G}$. In addition, it is assumed that there are inaccuracies in actual measurements, giving rise to $\hat{H}$. Thus the

estimator is

$$\dot{\hat{x}} = \hat{F}\hat{x} + \hat{G}u + K(z-\hat{z}) \tag{2.20}$$

$$\hat{z} = \hat{\bar{H}}\hat{x} + \hat{H}_2\hat{G}u \tag{2.21}$$

Substituting values of z and $\hat{z}$ into (2.20) yields

$$\dot{\hat{x}} = K\bar{H}x + [\hat{F} - K\hat{\bar{H}}]\hat{x} + [\hat{G}' + KH_2G]u + KH_2\Gamma w + Kv \tag{2.22}$$

with the definitions

$$G' \triangleq (I-KH_2)G \tag{2.23a}$$

$$\hat{G}' \triangleq (I-K\hat{H}_2)\hat{G} \tag{2.23b}$$

Using equations (2.1), (2.22), and the definition of the error in the state estimate $\tilde{x}=\hat{x}-x$, the error equation may be written

$$\begin{aligned}\dot{\tilde{x}} = {} & [(\hat{F}-K\hat{\bar{H}}) - (F-K\bar{H})]x + (\hat{F}-K\hat{\bar{H}})\tilde{x} \\ & + (\hat{G}' - G')u + Kv - \Gamma' w\end{aligned} \tag{2.24}$$

where

$$\Gamma' \triangleq (I-KH_2)\Gamma \tag{2.25}$$

Equation (2.24) shows the dependence of the estimator error on inaccuracies in the knowledge of the plant and measurement. Note that in each case, all $\bar{(\ )}$ and $(')$ quantities (e.g., $\bar{H}$, G') reduce to their standard definitions when $H_2=0$; i.e., the measurement is not a function of the derivatiaves of the states. The effects of the errors in G and H will be discussed in later sections as specific mechanizations are presented.

B. UNDISTURBABILITY

Breza and Bryson [2] have defined an undisturbable mode as one that is not controllable by the process noise, although it may be observable through the measurement. Using a Kalman filter such a mode would have a zero steady state filter gain indicating that the steady state filter pays no attention to the incoming measurement data and hence does not correct the initial estimate error of the mode. Undisturbable modes can be caused by pure integrations resulting either from modeling constant disturbances or from kinematic relationships in the state model. For example, the lateral equations of an aircraft with measurements of the roll and heading angles and process noise being a random lateral wind has an undisturbable heading mode. The filter thus has a neutrally stable eigenvalue which would cause the estimate of the heading mode to diverge.

One solution to this problem is to partition the system into undisturbable and disturbable modes, and then to design an optimal filter for the disturbable modes, and an observer with arbitrary dynamics for the undisturbable modes. A second method involves introducing aritificial process noise into the undisturbable modes. This second method was used in this work. The techniques of the previous section were used to determine the L matrix producing the reformulated problem. The $\bar{w}$ bar matrix was then modified so that the random lateral wind drove the state equations for roll and heading.

C. POLE ASSIGNMENT

In certain cases, optimal techniques produce estimators with relatively unpleasant characteristics. Most often, these are manifested by

unacceptably long time constants. The engineer has generally produced such a design by plugging estimated state and measurement noises into a design program, and is naturally unhappy with its consequences. He is faced with two choices: either to change the ratio of noises to produce a more desirable response, or to abandon optimal control entirely in favor of arbitrary pole placement. The former solution is made more difficult by the inapplicability of root square locus techniques for systems with more than one measurement. The relationship between noise ratios and eigenvalue movement is often not obvious. The pole placement technique, however, generally presents the designer with an overdetermined set of equations for the eigenvalues when there is more than one measurement. Estimator gains may be chosen by "closing the loop" with root loci or with other computer programs. Pole placement was used in the latter part of this work after being faced with slow response of certain variables.

III AIRCRAFT MODEL

The aircraft used for this study was the Piper PA-30. The equations of motion are those for straight and level flight.

1. Lateral Aircraft Model

The lateral equations of motion in body axes are [Systems Tech. Inc, 176-1, page C-3]:

$$\begin{bmatrix} \dot{v} \\ \dot{p} \\ \dot{r} \\ \dot{\phi} \\ \dot{\psi} \end{bmatrix} = \begin{bmatrix} Y_v & W_o & -U_o & g\cos\theta & 0 \\ L_v & L_p & L_r & 0 & 0 \\ N_v & N_p & N_r & 0 & 0 \\ 0 & 1 & \tan\theta & 0 & 0 \\ 0 & 0 & \sec\theta & 0 & 0 \end{bmatrix} \begin{bmatrix} v \\ p \\ r \\ \phi \\ \psi \end{bmatrix}$$

$$+ \begin{bmatrix} 0 & Y\delta_r \\ L\delta_a & L\delta_r \\ N\delta_a & N\delta_r \\ 0 & 0 \\ 0 & 0 \end{bmatrix} \begin{bmatrix} \delta_a \\ \delta_r \end{bmatrix} \qquad (3\text{-}1)$$

with the coefficients shown in Table 1. Note that all the aerodynamic terms are functions of density and velocity, with those in the control distribution matrix being a function of the square of velocity. The terms U_o and W_o are the components of the velocity vector along the body x and z axes respectively, stability axes not being assumed.

Table 1

LATERAL AERODYNAMIC COEFFICIENTS OF THE PA-30

$Y_v = \frac{S}{2m} \rho V C_{yB}$	$C_{yB} = -0.445$
$L_v = \frac{Sb}{2I_x} \rho V C_{\ell B}$	$C_{\ell B} = -0.0487$
$L_p = \frac{Sb^2}{4I_x} \rho V C_{\ell P}$	$C_{\ell P} = -0.47$
$L_r = \frac{Sb^2}{4I_z} \rho V C_{\ell r}$	$C_{\ell r} = 0.11$
$N_v = \frac{Sb}{2I_z} \rho V C_{nv}$	$Cn_v = 0.0756$
$N_p = \frac{Sb^2}{4I_z} \rho V C_{np}$	$Cn_P = -0.09$
$N_r = \frac{Sb^2}{4I_z} \rho V C_{nr}$	$Cn_r = -0.16$
$Y\delta_r = \frac{S}{2m} \rho V^2 C_{n\delta_r}$	$C_{y\delta_r} = 0.63$
$L\delta_a = \frac{Sb}{2I_x} \rho V^2 C_{\ell\delta_a}$	$C_{\ell\delta_a} = 0.0762$
$L\delta_r = \frac{Sb}{2I_x} \rho V^2 C_{\ell\delta_r}$	$C_{\ell\delta r} = -0.0115$
$N\delta_a = \frac{Sb}{2I_z} \rho V^2 C_{n\delta_a}$	$C_{n\delta_a} = 0.00281$
$N\delta_r = \frac{Sb}{2I_z} \rho V^2 C_{n\delta_r}$	$C_{n\delta_r} = -0.573$

$S = 178\ ft^2$	$I_x = 2800\ slug\text{-}ft^2$
$m = 111.9\ slugs$	$I_z = 4500\ slug\text{-}ft^2$
$b = 35.98\ ft^2$	

2. Longitudinal Aircraft Model

The linearized small perturbation equations of motion for the longitudinal mode are, in matrix form,

$$\begin{bmatrix} \Delta\dot{q} \\ \Delta\dot{w} \\ \Delta\dot{\theta} \\ \Delta\dot{u} \end{bmatrix} = \begin{bmatrix} M_q & M_{\dot{w}} & M_w & 0 & M_u \\ V_a + Z_q & Z_{\dot{w}} & Z_w & -g\sin\theta_o & Z_u \\ 1 & 0 & 0 & 0 & 0 \\ X_q & 0 & X_w & -g\cos\theta_o & X_u \end{bmatrix} \begin{bmatrix} \Delta q \\ \Delta w \\ \Delta w \\ \Delta\theta \\ \Delta u \end{bmatrix} + \begin{bmatrix} M_{\delta e} \\ Z_{\delta e} \\ 0 \\ X_{\delta e} \end{bmatrix} \begin{bmatrix} \Delta\delta_e \end{bmatrix} \qquad (3.2)$$

The following definitions for the dimensional derivatives appearing in (3.2) are used.

$$M_q = \frac{QSc}{I_{yy}} \frac{c}{2V_a} C_{mq} \qquad (3.3a)$$

$$M_{\dot{w}} = \frac{QSc}{I_{yy}} \frac{c}{2V_a} C_{m\dot{\alpha}} \frac{1}{V_a} \qquad (3.3b)$$

$$M_w = \frac{QSc}{I_{yy}} C_{m\alpha} \frac{1}{V_a} \qquad (3.3c)$$

$$M_u = \frac{QSc}{I_{yy}} C_{mu} \frac{1}{V_a} \qquad (3.3d)$$

$$M_{\delta e} = \frac{QSc}{I_{yy}} C_{m\delta e} \qquad (3.3e)$$

$$Z_q = \frac{QS}{m} \frac{c}{2V_a} C_{zq} \qquad (3.3f)$$

$$Z_{\dot{w}} = \frac{QS}{m} \frac{c}{2V_a} C_{z\dot{\alpha}} \frac{1}{V_a} \qquad (3.3g)$$

$$Z_w = \frac{QS}{m} C_{z\alpha} \frac{1}{V_a} \qquad (3.3h)$$

$$Z_u = \frac{QS}{m} C_{zu} \frac{1}{V_a} \qquad (3.3i)$$

$$Z_{\delta e} = \frac{QS}{m} C_{z\delta e} \tag{3.3j}$$

$$X_q = \frac{QS}{m} \frac{c}{2V_a} C_{xq} \tag{3.3k}$$

$$X_w = \frac{QS}{m} C_{xa} \frac{1}{V_a} \tag{3.3ℓ}$$

$$X_u = \frac{QS}{m} C_{xu} \frac{1}{V_a} \tag{3.3m}$$

$$X_{\delta e} = \frac{QS}{m} C_{x\delta e} \tag{3.3n}$$

The dimensionless coefficients which appear in Eqs. (3.3) are given in terms of the aircraft stability axes. The coefficients appearing in (3.3f) to (3.3n) are thus defined by the following nomenclature:

$$\begin{aligned}
C_{zq} &= -C_{Lq} \\
C_{z\dot{\alpha}} &= -C_{L\dot{\alpha}} \\
C_{z\alpha} &= -C_D - C_{L\alpha} \\
C_{zu} &= -2C_L - C_{Lu} \\
C_{z\delta e} &= -C_{L\delta e} \\
C_{xq} &= 0 \\
C_{x\alpha} &= C_L - C_{D\alpha} \\
C_{xu} &= -2C_D - C_{Du} \\
C_{x\delta e} &= -C_{D\delta e}
\end{aligned} \tag{3.4}$$

For straight and level flight, the lift coefficient is computed as

$$C_L = \frac{mg}{QS} . \tag{3.5}$$

From the value, the trim angle of attack can be found from

$$C_L = C_{L0} + C_{L\alpha}\, \alpha_{trim} . \tag{3.6}$$

In this study, for convenience it was assumed that the aircraft body axes were aligned with the aircraft stability axes for each steady flight condition examined. Stability derivatives were computed for several flight conditions; these were subsequently used in the study. Pertinent values of the coefficients and derivatives are listed in Table 2. The approach flight speed was computed as

$$\begin{aligned} V_{approach} &= 1.3\, V_{stall} + 0.5\ (\text{surface winds}) + (\text{reported gusts}) \\ &= 147 \qquad + 0.5\ (33) \qquad + 12.5 \\ &= 176\ \text{ft/sec.} \end{aligned} \tag{3.7}$$

Cruise speed was assumed to be 185 kts (304 ft/sec). An intermediate speed of 165 kts (279 ft/sec) was also used. Altitudes of 0, 1500 ft, and 5000 ft were assumed at various points in the investigation.

Other pertinent data for the PA-30 aircraft include:

$$S = 178\ ft^2$$

$$c = 5\ ft$$

$$I_y = 1900\ lb \cdot ft \cdot sec^2$$

$$A = 7.28$$

$$e = 0.88$$

$$C_{L0} = 0.33$$

Table 2

STABILITY DERIVATIVES OF THE PIPER PA-30 FOR VARIOUS FLIGHT CONDITIONS

Set No.	1	2	3	4	5
V_a: ft/sec^{-1}	176	279	304	304	304*
h: f	30	5000	0	5000	0
ρ: lb.s^2.ft	0.002377	0.002048	0.002377	0.002048	0.002377
Q: lb	36.81	79.71	109.83	94.64	109.83
M_q: s^{-1}	-3.429	-4.684	-5.923	- 5.104	-6.516
M_w: ft^{-1}s^{-1}	-0.04660	-0.07668	-0.09697	-0.08355	-0.1212
M_u: ft^{-1}s^{-1}	0	0	0	0	0
$M_{\delta e}$: s^{-2}	-32.62	-75.95	-100.16	-88.90	-120.19
Z_q: ft.s^{-1}	7.14	9.78	12.37	10.71	15.46
Z_w: s^{-1}	-1.388	-1.769	-2.236	-1.927	-2.348
Z_u: s^{-1}	-0.3613	-0.2306	-0.2117	-0.2117	-0.2011
$Z_{\delta e}$: s^{-2}	-67.15	-159.83	-270.28	-215.64	-337.85
X_q: ft.s^{-1}	0	0	0	0	0
X_w: s^{-1}	0.10660	0.07099	0.06516	0.06516	0.06190
X_u: s^{-1}	-0.03061	-0.02191	-0.02667	-0.02298	-0.03333
$X_{\delta e}$: s^{-2}	0	0	0	-	0

*Derivative set based on typical flight test uncertainty [4, 5].

IV. SURVEY OF INSTRUMENTS

The survey of linear and angular accelerometer, angular rate sensors, magnetometers, absolute and differential pressure transducers, linear and angular position transducers, as well as a few temperature sensors is essentially completed. Tables presenting relevant data for one or more models of each manufacturer are attached as Appendix A. Additional data for all models listed, as well as data on other models made by each manufacturer but not listed is on file. In some sensor types, silicon technology is here, whereas in others, development is still short of the possible goal of adequate performance at very reduced cost. Low cost, reliable sensors of any type would satisfy the goals of the study. The state of the art in reaching that point is variable. Each category of instrument warrants some discussion.

Linear Accelerometers. The available units surveyed range in price from $120 to $595 in small quantity with $50 in 1000 quantity being the lowest available price. This undamped Entran unit is a cantilever beam type with semiconductor strain gage (piezoresistive) half bridge readout. The very high thermal bias sensitivity (5g/100°F) is one of its disadvantages. This number is more than 3000 times worse than that of the Teledyne FP 1. Of about 30 types included, only four give data on expected life. At least four companies making triaxial units were included in the survey; Entran, Setra, Humphrey, (the Donner 4384 is single axis), and Donner. The Setra 113 triaxial is available at $142 per axis in small quantities. Silicon transducers are under development but are marginal at the present time. Flight data should be obtained with conventional instruments.

Angular Accelerometers. Only three companies surveyed make angular accelerometers. Of these, one makes units ranged too high (10^3 to 10^4 rad/sec^2); another (Donner) makes units selling for $2500 in quantities of 100 to 500, but the third (Schaevitz) makes suitable units selling at about $500 in 100-200 quantities. All but the first are listed.

Linear accelerometers could be used to measure angular accelerometers, in principle; but the performance requirements are too exacting to make them competitive for the proposed application. For further discussion, see App. B.

This is the least probable area in which silicon technology is likely to provide a quick solution to high cost at an adequate performance.

Angular Rate Sensors. Only three companies have been found making rate sensors. The Donner 8160 is presently used in many commercial jet aircraft for rate gyro replacement. It is the angular accelerometer with electronic integration. The Humphrey devices (manufactured under license from Hercules, Inc.) is a true rate sensor using a gas jet passing between parallel hot wires. Our data on the B.A.C. Ltd unit is very sketchy at present.

While these rate sensors may be acceptable in performance, the initial cost appears too high for general aviation even though it is justified for commercial aircraft on the basis of reduced maintenance. At the present time, rate gyros may be a better interim solution.

Magnetometers. Of 15 companies claiming to manufacture magnetometers surveyed, only five offer units which are suitable for this application. Most of the others are for geological sample testing.

All of the listed units are of the fluxgate type with three of the five being triaxial. These three have a common origin in a rocket flight magnetometer application for which NASA Goddard issued contracts with a common specification. This accounts for the similarity of these units. The lowest priced unit listed (Infinetics) is not satisfactorily covered with specifications as its normal use is weapon detection for airport security; however, the manufacturer has indicated that they should be capable of our requirements if calibrated. The per axis price is a factor of 5 to 6 lower than the triaxial units.

Flight test data are needed here more than for any other instrument. They have not been used in aircraft as a vector reference before. The data available is generally just heading and then that is smoothed with a gyro. The more expensive nulled (feedback) instruments have adequate performance, but may be degraded by aircraft installation problems. It remains to be seen if the lower cost units will hold calibration adequately. New algorithms are to be evaluated, and real data must be used to obtain reliable results.

Absolute Pressure Transducers (altitude). The attached Tables, App. A, compares transducers made by 22 companies. Accuracy is given as a percent ful scale in various categories. The sea level altitude error was calculated as a root sum squared combination of static error (which includes linearity, hysteresis, and repeatability), thermal bias shift for a $\pm$ 50°F deviation. In cases where a combined thermal error was given, this was used in root sum squared combination with static error as defined above. In some cases, the available data was not sufficient to permit the calculation. Items not included in the sea level altitude error calculation were long term stability due to insufficient data and initial zero balance which would be trimmed out. It was of course assumed that the local barometric correction was made by the pilot. Four of the transducers listed provide the functionalization required to obtain an output linearilly proportional to altitude. These are the Rosemount 1241A and 542kl, the Bourns 200-438-1002, and of course the Honeywell HG 280 air data computer system. In all other cases, the functionalization is a user responsibility. The Rosemount 542K1 and 542K2 provide both direct airspeed (IAS) and dynamic pressure (q_c), in addition to direct altitude (h) the only difference being the airspeed range. Some improvement is possible with the low priced sensors by calibrating each sensor against nonlinearity and temperature by least squares fitting. However, the tradeoff of this against buying a more accurate sensor needs further study.

An alternative to the use of an altitude pressure transducer would be to increase the resolution of the optical encoder presently used with altitude encoding altimeters by a factor of 10 such that 10 ft resolution is available. This approach could lead to a less expensive means of obtaining the data.

The silicon technology is not here yet for altitude measurement. The required improvement in performance is very large. A conventional instrument must be used unless and until there is a change in the state of the art.

Differential Pressure Transducers (airspeed). The Table (App. A) compares 21 transducers made by 17 companies. Airspeed ranges for the units considered vary; however, in general, most companies will supply any range desired. Accuracies are given as static error (defined above), thermal bias error, and thermal sensitivity error. Although airspeed error is not estimated in the Table it can be calculated approximately by combining the sources of pressure error as desired to obtain a composite pressure error and then using the following relationship:

$$\text{error(knots)} = \frac{(\text{range knots})^2}{\text{airspeed knots}} \times \frac{\text{PSID\% error}}{2} \times 10^{-2} .$$

For example, a sensor with a 2 PSID (285 knots) range, and 0.5% composite pressure error gives an airspeed accuracy at 100 knots of ±2 knots. Three of the transducers listed provide the functionalization required to obtain an output linearly proportional to airspeed. These are the Rosemount 542K2, the Bourns 200-538-1002, and the Honeywell HG 280 air data computer. The methods of functionalization, as well as cost and performance, are dramatically different for these three device-types as is illustrated below:

Device	Functionalization Method	Accuracy* -50-150°F (knots)	Cost
Bourns 538 (IAS) 438 (h)	nonlinear pot	(IAS) ±8k at 100 k (h) ±825 ft. S.L.	$755
Rosemount 542K2	Analog Electronics	(IAS) ±3k at 100 k (h) ±47 ft at S.L. (q_c) 0.5 to 1.5%	$2,360
Honeywell HG-280 Digital Air Data Computer	Many functions provided. Used in DC 10	(CAS) ± 2k at 100 k (h) ± 30 ft at S.L. (Mach) ± 0.005 at 0.35	$15,000 to $20,000

* at sea level (S.L.)

Low cost silicon sensors should prove acceptable. The airspeed display can be nonlinear. There may not be a significant requirement for functional fitting because it is the dynamic pressure which is measured which is of interest in most cases.

Linear Displacement Transducers. This Table compares linear displacement transducers made by 18 companies. The transducers surveyed are of various types and cover strokes ranging from $\pm$ 0.005 inches to 500 inches at prices from $32.00 to $700.00, in small quantities. Actuation force ranges from 6.5 lb/in. for some spring loaded units to essentially zero for free slug LVDT (linear voltage differential transducer) units. Kavlico has applied many types of LVDT units to commercial and military aircraft applications with results like $< 15 \times 10^6$ revenue flight hours without a single operational failure.

Angular Displacement Transducers. Although angular displacement transducers were not directly surveyed, many of the companies sent literature in angular displacement devices such as potentiometers, LVDTs (linear variable differential transformers), encoders, and beam deflection with strain gage (linked to shaft rotation). In addition, there are many types of resolvers and synchros available for this application. Examples of leading companies manufacturing these components are shown below.

Angular Transducer Type	Company
potentiometer (pot)	Bourns Spectral TRW Dale
LVDTs	Schaevitz Kaulico
Encoders	Astrosystems Baldwin Clifton/Litton Singer/Kearfott
Beam Deflection	West Coast Research
Resolver/Synchro	Singer/Kearfott Bendix Clifton/Litton

A. METHODS FOR TESTING CANDIDATE TRANSDUCERS

The following methods are planned for testing the candidate transducers. In some cases, the tests are simpler than conventional testing methods. Most of the tests will be performed at Stanford, however, facilities for some types of transducers are not conveniently available on campus and we plan to use nearby facilities.

Linear Acceleration

We are currently evaluating some accelerometers. We are using two testing methods. The first is the standard gravity test signal on a dividing head. A Leitz dividing heas is used which gives 10^{-5} rad accuracy and hence provides us with two axes of orientation of the instrument with respect to gravity and enables us to do some cross coupling and nonlinear testing in addition to scale factor and bias. The second testing method is on a shaker which lets us look at nonlinear terms for higher g. We also look at harmonic content generated and wave shape distortions for large signals. Depending upon the nature of the instrument output, more or less calibration work will be done on each of these facilities depending upon the nature of the information to be sought.

Angular Accelerometers and Angular Rate Sensors

We have decided to do the evaluation of both these types of instruments on a torsional shaker. Adequately large signals are available on the one in our laboratory at Stanford. It has a 0 to $\pm$ 15 deg amplitude, at a frequency that can be chosen between 0 and 30 Hz. An optical method will be used to determine the peak amplitude. Hence, angular velocities an order of magnitude larger than we expected to see in an aircraft, are available and considerably higher accelerations than are of interest can be generated. Because the angular accelerometers and rate sensors are to be used in combination with magnetometers and accelerometers which will be the primary source of long term orientation information, no conventional gyro drift test will be performed.

Magnetometers

Testing magnetometers require a large, complicated facility. Stanford has no such facility but there is a very good one at NASA Ames that we should be able to use. There they are able to measure magnetometer zero offset, linearity, and drift; and they routinely run tests on flux-gate magnetometers of the type we are considering.

Air Data Sensors

Air data sensors, including absolute and differential pressure transducers, are usually tested using precision servo controlled pressure sources. There are several adequate test facilities in the Bay Area, including one at NASA Ames. If necessary, an acceptable system could be purchased for $10,000 to $15,000. Another alternative would be to use the local instrument shops that serve the general aviation community, but their equipment may not have the required accuracy.

Linear Displacement

The work table of a sip jig borer, which is calibrated to very high precision, is a very convenient work table on which to do displacement calibration work. We have had very good success in calibrating LVDTs using this setup in the past.

Angle Transducers

Conventional dividing heads should provide adequate accuracy for calibrating angle transducers. If interest develops, a Leitz dividing head good to 10^{-5} rad is available for especially fine measurements.

B. MICROPROCESSOR INTERFACE CONSIDERATIONS

The interface between the aircraft sensors and the microprocessor can be either high level d-c analog or bit parallel digital. For analog signals, an A/D converter controlled by the microprocessor must be used. To digitize more than one analog input, a processor controlled analog multiplexer must be connected to the A/D converter. Most A/D converters require a fairly high level input of 0 ± 1 V to 0 ± 10 V. Sensors that produce signals smaller than this will require some signal conditioning prior to conversion. Sensor that produce a-c signals will probably require demodulation to produce a d-c signal for the converter. Actually most A/D converters are fast enough to do the demodulation under software control but this often uses a lot of processor time and is undesirable unless the processor is lightly loaded. In any case, the hardware for d-c or a-c signal conditioning is straightforward except for sensors that produce very small signals. Sensors with digital outputs can be connected directly to the microprocessor's I/O bus through an appropriate buffer. This buffer gates the data on to the 8 bit to 16 bit wide I/O bus under processor control.

The actual hardware that must be purchased and/or developed depends on the number of sensors and the type of μprocessor used. Some of the converter-producing companies sell complete data acquisition systems that plug directly into the chassis of some established μprocessors such as the popular Intel 8080. These printed circuit boards are completely compatible with the μprocessor and require no hardware development by the user. A typical system with 16 analog inputs and 12 bit digital resolution costs about $700 in single quantities and $300 for 100 units. This class of μprocessor uses 8 bits words and has limited arithematical capability and may not be powerful enough for our application.

The recent more powerful μprocessors such as the one used in the H-P 9825 and the Data General micro NOVA approach minicomputer sophistication. Processors such as these used 16 bit words and have powerful arithmetic logic, but compatible plug-in data acquisition systems are not yet available. What is available, however, are digital I/O boards which provide a well defined, fairly simple digital interface to the user. To these boards can be connected A/D converters, multiplexers, etc., with a small number of logic integrated circuits. Some converter companies produce data acquisition modules that contain the multiplexer, the A/D converter, and some control logic which can be connected to the digital I/O boards with even less logic. In either case the user must do some logic design and is responsible for the compatibility of the digital and analog subsystems. Digital I/O boards or modules are supplied by the μprocessor manufacturer and cost $200 to $400 in single quantities. A typical 16 analog input, 12 bit data acquisition module costs $300 in single quantities and about $150 for 1000 units.

The amount of hardware design required for such an interface depends strongly on the data rate. The above discussion assumed that data was gathered in the simple programmed I/O mode. This mode requires simple hardware but uses a lot of processor time. Data rates of 10 to 5000 total samples/sec (e.g., 1 to 500 samples/sec for each of 10 sensors) are reasonable depending on the processor work load. To define a tighter data rate range would require knowledge of a specific processor and the software tasks. The program interupt mode of data gathering requires somewhat more interface hardware but uses less processor time and thus allows higher data rates. The Direct Memory Access (DMA) mode requires still more hardware but uses very little processor time and allows data rates up to the maximum capability of the A/D converter—up to 100,000 samples/sec. Most μprocessors support all three modes of data input. The appropriate mode depends entirely on the application. The interface for any of these modes uses standard integrated circuits and the entire analog input subsystem is far less complicated then and should be at least as reliable as the μprocessor itself.

V

STATE ESTIMATOR DESIGN FOR THE LONGITUDINAL MODE*

In the longitudinal mode, the two aircraft state variables which are not considered to be directly measureable are the pitch attitude θ, and the pitch rate q. The objective of the state estimator is to determine estimates of these variables as well as to produce smoothed values of the other variables which are directly measured. The smoothing is desired to reduce the effects of instrument noise and wind disturbances on the sensor signals.

A. OBSERVER DESIGN

The linearized aircraft perturbation equations for longitudinal motion, including wind and instrument dynamics, are given in Eqs. (3.2). In abbreviated form, these equations are represented by the matrix differential equation

$$\dot{x} = Fx + G_1 u + \Gamma \eta_1 \ . \tag{5.1}$$

Here,

x = state vector,

u = control input vector,

η_1 = wind noise vector,

F = system dynamics matrix,

G_1 = control distribution matrix,

Γ = wind distribution matrix.

---

* The material of this chapter was taken from Ref. 8.

The estimator model is

$$\dot{\hat{x}} = \hat{F}\hat{x} + \hat{G}u_m + K(y - \hat{y}) \quad . \tag{5.2}$$

Here,

$\hat{x}$ = estimated state vector,

u_m = measured control input vector,

$\hat{F}$ = assumed system dynamics matrix,

$\hat{G}$ = assumed control distribution matrix,

and measurement y is

$$y = Hx + \eta_2 \quad . \tag{5.3}$$

H is the output distribution matrix, and η_2 indicates measurement noise. To obtain an error signal, an estimate of the measurement $\hat{y}$ is formed:

$$\hat{y} = \hat{H}\hat{x} \quad . \tag{5.4}$$

In almost all flight control applications, it is necessary to have the estimator produce θ, q, and h. A full state estimator in $\Delta\hat{q}$, $\Delta\hat{w}$, $\Delta\hat{\theta}$, $\Delta\hat{u}$, plus altitude perturbation Δh is therefore desirable. In addition, it is possibly desirable to estimate winds, $(\hat{w}x, \hat{w}z)$, lagged instrument measurements, $(\Delta\hat{u}_m, \Delta\hat{h}_m)$, and instrument biases, $(b_{az}, b_u, b\delta_e)$.

The full ten-state estimator mechanized here used 10 gains with 3 measurements: 4 gains associated with the vertical accelerometer, 4 with the measurement of airspeed, and 2 with altitude measurement. In determining the estimator gains, the coupling between the short-period and phugoid equations was ignored; the associated gains were selected independently. The coupling was included in the actual estimator mechanization however.

The equations of the short-period mode, phugoid mode, and altitude kinematics were combined along with equations for wind components and certain biases to produce the ten-state estimator where

$$\hat{F} \triangleq \left[\begin{array}{cccc|cccc|cc} \hat{M}_q & \hat{M}_w & \hat{Y}_{1z} & 0 & 0 & \hat{M}_u & 0 & \hat{Y}_{1x} & 0 & 0 \\ \hat{V}_a+\hat{Z}_q & \hat{Z}_w & \hat{Y}_{2z} & 0 & -g\sin\hat{\theta}_o & \hat{Z}_u & 0 & \hat{Y}_{2x} & 0 & 0 \\ 0 & 0 & -\hat{d}_z & 0 & 0 & 0 & 0 & 0 & 0 & 0 \\ 0 & 0 & 0 & 0 & 0 & 0 & 0 & 0 & 0 & 0 \\ \hline 1 & 0 & 0 & 0 & 0 & 0 & 0 & 0 & 0 & 0 \\ \hat{X}_q & \hat{X}_w & \hat{Y}_{4z} & 0 & -g\cos\hat{\theta}_o & \hat{X}_u & 0 & \hat{Y}_{4x} & 0 & 0 \\ 0 & 0 & 0 & 0 & 0 & \hat{d}_u & -\hat{d}_u & -d_u & 0 & 0 \\ 0 & 0 & 0 & 0 & 0 & 0 & 0 & -d_x & 0 & 0 \\ \hline 0 & -\cos\hat{\theta}_o & 0 & 0 & \hat{V}h_o & \sin\hat{\theta}_o & 0 & 0 & 0 & 0 \\ 0 & 0 & 0 & 0 & 0 & 0 & 0 & 0 & \hat{d}_h & -\hat{d}_h \end{array}\right] \tag{5.5}$$

$$K^T = \begin{bmatrix} K_1 & K_2 & K_3 & K_4 & 0 & 0 & 0 & 0 & 0 & 0 \\ 0 & 0 & 0 & 0 & K_5 & K_6 & K_7 & K_8 & 0 & 0 \\ 0 & 0 & 0 & 0 & 0 & 0 & 0 & 0 & K_9 & K_{10} \end{bmatrix} \tag{5.6}$$

The ten state variables for this estimator are:

$$x^T = [\Delta q,\ \Delta w,\ W_z,\ b_{az},\ \Delta\theta,\ \Delta u,\ \Delta u_m,\ W_x,\ \Delta h,\ \Delta h_m]. \tag{5.7}$$

A five-state estimator without wind or bias terms was also tested extensively.

Runs were made to compute and plot the transient state estimate errors $\tilde{x}$ ($\tilde{x} = x - \hat{x}$) due to modeling errors and estimate initial condition errors. Modeling errors were simulated based on stability derivatives in the observer set for a different altitude and airspeed than those set for the actual aircraft flight conditions. In one set of cases, $\hat{V}_a$ of the estimator and the associated derivatives were based on an assumed nominal airspeed of 100 kts. The nominal V_a ($V_{a_{nom}}$) was assumed to be 185 kts. Thus, the stability derivatives used to model the actual aircraft motion were based on airspeed of 185 kts. The airpseed perturbation Δu which was assumed as the measurement to this system was $\Delta u = V_a - V_{a_{nom}}$. Plots of transient errors $\Delta\tilde{q}$, $\Delta\tilde{\theta}$, and $\Delta\tilde{h}$ due to errors in the observer estimate initial conditions with these gross modeling errors

revealed that although the ten-state observer produces a smaller pitch rate error $\Delta\tilde{q}$, the pitch angle $\Delta\tilde{\theta}$ and attitude $\Delta\tilde{h}$ errors are smaller for the five-state system. The reason for this is that when there are extra wind states with incorrect models, the observer takes measurement differences and partially converts these to wind estimates. The conclusion is that extra states improve performance only if the modeling is correct.

For transients due to an elevator input sequence consisting of a 3° doublet over 0.8 sec followed by a 0.3° step input lasting through 10 sec, the five-state estimator produces superior performance in estimating the vertical and longitudinal airspeed components (Δw, Δu) and pitch angle $\Delta\theta$. Pitch rate $\Delta\tilde{q}$ and altitude $\Delta\tilde{h}$ errors are about the same for both observers. Again, the five-state observer proves to be overall more tolerant of modeling errors.

From results with estimators containing modeling errors, the following general conclusions can be made:

1. Observers with fewer states are less susceptible to modeling errors. Adding states to the observer to increase its accuracy should only be done when a good overall model is known and used.

   The pitch angle error transients for the ten-state observer with initial estimate errors and elevator inputs are totally unacceptable. The pitch angle error transient for the five-state observer was excessive only during a gust. Thus, it is recommended that the five-state observer be used as a first choice flight for test purposes.

2. The stability and control derivatives are a function of airspeed. It is recommended that the values used for these derivatives be updated to match the airspeed as closely as is practical.

The effects of mismodeling were very serious--the stability derivatives varying with velocity, and the control derivatives varying with the square of velocity. To reduce these effects, the mechanized values of the derivatives were changed with airspeed and altitude (all derivatives are functions of density) and the following results obtained.

1. Dividing the flight speed range into finite regimes is an effective way to reduce modeling errors. It provides a simple way to implement gain changes. For the PA-30, dividing the span of flight speeds into three segments is adequate. Altitude change effects are not important.

2. The control derivatives are more sensitive to speed changes than are the other parameters. It is recommended that these quantities be updated for every 10 ft/sec change in flight speed.

3. The effect of uncertainties in the dimensionless stability derivatives can be significant, especially on the pitch angle error. Careful modeling is necessary, and the effects of known uncertainties on the results should be checked. This factor is a strong motivation for careful parameter identification of the derivatives. This is most important for the control derivatives, $M_{\delta e}$ and $Z_{\delta e}$.

B. KINEMATIC FILTER DESIGN

For the longitudinal mode of the aircraft, body-mounted translational and rotational accelerometers would measure the perturbation quantities

$$\begin{aligned} \Delta a_{xm} &= \Delta\dot{u} + \qquad + g \cos\theta_o \, \Delta\theta + \eta_{ax} , \\ \Delta a_{zm} &= \Delta\dot{w} - V_a \Delta q + g \sin\theta_o \, \Delta\theta + \eta_{az} , \\ \Delta\dot{q}_m &= \Delta\dot{q} + \eta_{\dot{q}} . \end{aligned} \tag{5.8}$$

Accelerometer measurement errors are indicated by the terms η_{ax}, η_{az}, and $\eta_{\dot{q}}$. Note that these equations contain primarily the kinematic terms V_a, and θ_o; the aerodynamic forces and moments are not explicitly modeled. These equations can be transformed to

$$\Delta\dot{u} = \Delta a_{xm} - \quad - g \cos\theta_o \Delta\theta ,$$

$$\Delta\dot{w} = \Delta a_{zm} + \quad \Delta q - g \sin\theta_o \Delta\theta , \tag{5.9}$$

$$\Delta\dot{q} = \Delta\dot{q}_m .$$

Here, the error terms are neglected. These equations form the basis for constructing an alternate state estimator which does not require specific aircraft modeling as with the observer approach. It is noted that mechanization of this state estimator approach does not have to be based on small perturbation assumptions, as with the previously discussed observer approach. However, the small perturbation assumptions and notation are maintained to allow linear analysis and direct comparison between the two approaches.

To these equations, the kinematic expressions

$$\Delta\dot{\theta} = \Delta q$$

$$\Delta\dot{h} = -\cos\theta_o \Delta w + Vh_o \Delta\theta + \sin\theta_o \Delta u \tag{5.10}$$

are added. Here, Vh_o is $V_a \cos\theta_o$. These are the equations of the state estimator considered here. In (5.9), the measured acceleration (Δa_{xm}, Δa_{zm}, and $\Delta\dot{q}_m$) are treated as inputs (like the elevator position inputs for the observer approach). Because (5.9) and (5.10) are made up of measured accelerations and kinematic terms, this filter concept is referred to as a "kinematic filter."

In matrix form, the kinematic filter is implemented as follows:

$$\begin{bmatrix} \Delta\dot{\hat{q}} \\ \Delta\dot{\hat{w}} \\ \Delta\dot{\hat{\theta}} \\ \Delta\dot{\hat{u}} \\ \Delta\dot{\hat{h}} \end{bmatrix} = \begin{bmatrix} 0 & 0 & 0 & 0 & 0 \\ V_a & 0 & -gs\theta_o & 0 & 0 \\ 1 & 0 & 0 & 0 & 0 \\ 0 & 0 & -gc\theta_o & 0 & 0 \\ 0 & -c\theta_o & V_{ho} & s\theta_o & 0 \end{bmatrix} \begin{bmatrix} \Delta\hat{q} \\ \Delta\hat{w} \\ \Delta\hat{\theta} \\ \Delta\hat{u} \\ \Delta\hat{h} \end{bmatrix} + \begin{bmatrix} 1 & 0 & 0 \\ 0 & 1 & 0 \\ 0 & 0 & 0 \\ 0 & 0 & 1 \\ 0 & 0 & 0 \end{bmatrix} \begin{bmatrix} \Delta\dot{q}_m \\ \Delta a_{zm} \\ \Delta a_{xm} \end{bmatrix} + \begin{bmatrix} K_{11} & 0 \\ K_{21} & K_{22} \\ K_{31} & 0 \\ K_{41} & 0 \\ 0 & K_{52} \end{bmatrix} \begin{bmatrix} \Delta U_m - \Delta\hat{u} \\ \Delta h_m - \Delta\hat{h} \end{bmatrix} \tag{5.11}$$

Note that the airspeed measurement Δu_m is not used to update the altitude estimate $\Delta\hat{h}$, and the altimeter measurement Δh_m is not used to update estimates of $\Delta\hat{q}$, $\Delta\hat{\theta}$, or $\Delta\hat{u}$. This naturally follows from the orthogonality of the equations. Thus, only six gains are required to implement this state estimator. The gain K_{21} can also be eliminated, and this results in the gain selection for the vertical motion being decoupled from the forward and pitch motion.

The obvious advantage of the kinematic filter over the observer is that no aerodynamic stability derivatives need to be modeled. Also, elevator deflection measurements (δ_e) aren't required. The immediate disadvantage, from the mechanization point-of-view is that angular accelerometer and forward linear accelerometer measurements are required.

Testing this kinematic filter resulted in the following conclusions.

1. The dominant disturbance affecting the estimate was the longitudinal wind gust. The kinematic filter produces about the same error for $\Delta\hat{u}$ as the observer, slightly larger errors for $\Delta\hat{q}$ and $\Delta\hat{\theta}$, and substantially larger errors for $\Delta\hat{w}$. These error sensitivities are, of course, dependent on the filter gains, and a tradeoff exists between steady state error and transient response.

2. Of the instrument noise errors, only the angular accelerometer noise produced a significant effect. Some prefiltering may be warranted.

3. The only significant modeling error that can occur in the kinematic filter formulation is using an incorrect value for the nominal airspeed. In all cases, errors resulting from an incorrect mechanized value of airspeed were only slightly greater than if the correct value was used. The kinematic filter is much less sensitive to modeling errors than the aerodynamic observer.

VI LATERAL ESTIMATOR

The lateral equations of state are shown in equation (3.1). The states are lateral velocity, roll rate, yaw rate, roll angle, and heading. Currently, steady-state heading is determined using a magnetic compass, and short-term heading changes are displayed by a directional gyroscope. In IFR flight, the directional gyro is reset by the pilot to agree with the compass every 10 to 15 minutes in level flight, and before each approach to landing. The primary attitude reference is the artificial horizon that displays pitch and roll angles. Another gyroscope displays rate of turn (yaw rate). The simplest of all instruments, a damped ball in a curved tube, indicates lateral coordination. Ignoring this passive instrument the pilot's lateral displays are roll angle, heading, and yaw rate.

Aerodynamic Model Observer

Quantities that can be sensed for use in the lateral estimator are: heading, yaw rate, yaw angular acceleration, roll angle, roll rate, roll angular acceleration, lateral velocity, and lateral acceleration. The scope of this work requires that angular velocities not be considered, they being measurable primarily with gyroscopes. Lateral velocity will also be ruled out as it is measurable primarily with lateral angle of attack vanes; in addition, the design of an observer would not ordinarily choose lateral velocity as a measurement, inasmuch as it does not play a major role in the observability of the system. In considering which (if any) of the acceleration measurements should be used, the price and complexity of the instruments must be taken into account. Linear accelerometers are the least

complex and costly, and inasmuch as lateral acceleration is used as a measure of coordination, it is a reasonable measurement. The inclusion of roll or yaw angular acceleration will depend on which angles measured. If both roll and yaw (heading) are measured, both angular velocities are determined, and thus, the measurement of the accelerations will just add a high frequency component to the observer. If roll is not measured, the measurement of roll acceleration will add important information to the observer as roll will be derived only through the other observed equations. Inas much as yaw must be measured to provide the "outer loop" measurement to the entire observer, it is reasonable to measure roll rate. Thus, for an observer in which the dynamics of the system are modelled, the observations chosen are heading, lateral acceleration, and roll acceleration.

The equations of such an observer are

$$\begin{bmatrix} \dot{\hat{v}} \\ \dot{\hat{p}} \\ \dot{\hat{r}} \\ \dot{\hat{\phi}} \\ \dot{\hat{\psi}} \end{bmatrix} = \begin{bmatrix} Y_v & W_o & -U_o & g\cos\theta & 0 \\ L_v & L_p & L_r & 0 & 0 \\ N_v & N_p & N_r & 0 & 0 \\ 0 & 1 & \tan\theta & 0 & 0 \\ 0 & 0 & \sec\theta & 0 & 0 \end{bmatrix} \begin{bmatrix} \hat{v} \\ \hat{p} \\ \hat{r} \\ \hat{\phi} \\ \hat{\psi} \end{bmatrix}$$

$$+ \begin{bmatrix} 0 & Y\delta_r \\ L\delta_a & L\delta_r \\ N\delta_a & N\delta_r \\ 0 & 0 \\ 0 & 0 \end{bmatrix} \begin{bmatrix} \delta_a \\ \delta_r \end{bmatrix} + [K] \begin{bmatrix} z_1 - Y_v\hat{v} - Y\delta_r\delta_r \\ z_2 - L_v\hat{v} - L_p\hat{p} - L\delta_a\delta_a - L\delta_r\delta_r \\ z_3 - \hat{\psi} \end{bmatrix} \tag{6.1}$$

with three measurements:

$z_1 = a_y$, the lateral linear acceleration,

$z_2 = \alpha_x$, the roll angular acceleration,

$z_3 = \psi$, the magnetic heading.

Note in equation (6.1) that since measurements 1 and 2 are derivatives of states, the control appears in the term $K(z-\bar{H}\hat{x})$. Such an observer may be designed using methods of optimal control by first calculating the decoupling matrix L of Section II from the estimated measurement and plant noise covariances. The equivalent system $(\bar{F},\bar{G},\bar{H})$ may be used in an eigenvalue decomposition program such as OPTSYS to find the optimal gain matrix $\bar{K}$. The actual gain used in the estimator is $(\bar{K}+L)$. This procedure was performed for the PA-30 aircraft for a variety of covariances at an airspeed of 176 ft/sec. At this speed, the roots of the aircraft are:

-3.96 sec^{-1}, roll subsidence

-5.49 ± 2.14 sec^{-1}, Dutch roll

0.00233 sec^{-1}, spiral divergence

and a root at the origin representing heading.

An observer with good transient behavior has roots at: -1.64, -1.02, $\pm.759$, $-.140 \pm .150$ sec^{-1}.

Perhaps as important as behavior of the estimator to transients and wind gusts is its behavior when the aircraft receives a control input from the ailerons or rudder. This can be considered separately from transient behavior due to superposition of responses. The response of the estimator error, equation (2.24), to control inputs, is obviously dependent on the

knowledge of $G'=(I-KH_2)G$ as well as the actual control u. It can be seen from Table 1 that the elements of G are a function of dynamic pressure; i.e., air density and the square of speed. Thus, any error in the knowledge of the aircraft's speed with manifest itself in an error in the mechanization of G and thus give rise to an effect on the observer by a control input. Unless the mechanization updates the aircraft speed constantly and recalculates the mechanized values of G, this error will exist. In addition, the terms in the elements of G that are aircraft dependent are typically the least understood theoretically of all stability derivatives although empirical data is reliable.

To determine the effect of this mismatch, a 15 second digital simulation was performed in which the aircraft was subject to a single square-wave input in aileron of amplitude 0.1 radian and 10 second period (with no forcing term for the last 5 seconds). The aircraft speed is 176 ft/sec; the estimator is mechanized assuming an aircraft going at 150 ft/sec.

Figures 6.1a-e show the response of the aircraft along with the estimator errors. The errors are clearly unacceptable. They can be explained by examining equation (2.24). The observer error is a function of the mismatch G (which is a function of the square of velocity) multiplied by observer feedback gain. The term $KH_2(\hat{G}-G)$ may be large (N.B. this large term exists only in an observer with nonzero H_2; i.e., where there is observation of state derivatives.) Parenthetically, it can be noted that the effect of this term reduces to zero if $(I-KH_2)=0$, a condition that is unlikely to be met in a stable system. Work by the experimenter has failed to reveal a system with acceptable transient behavior (roots) in which the response to control modeling error is small.

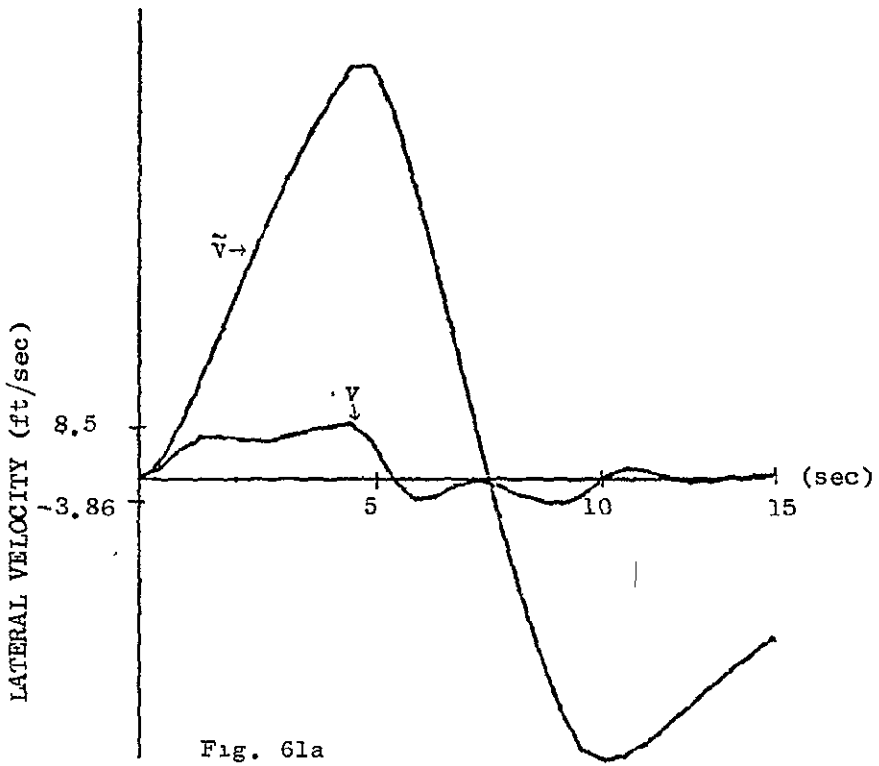

Fig. 6la

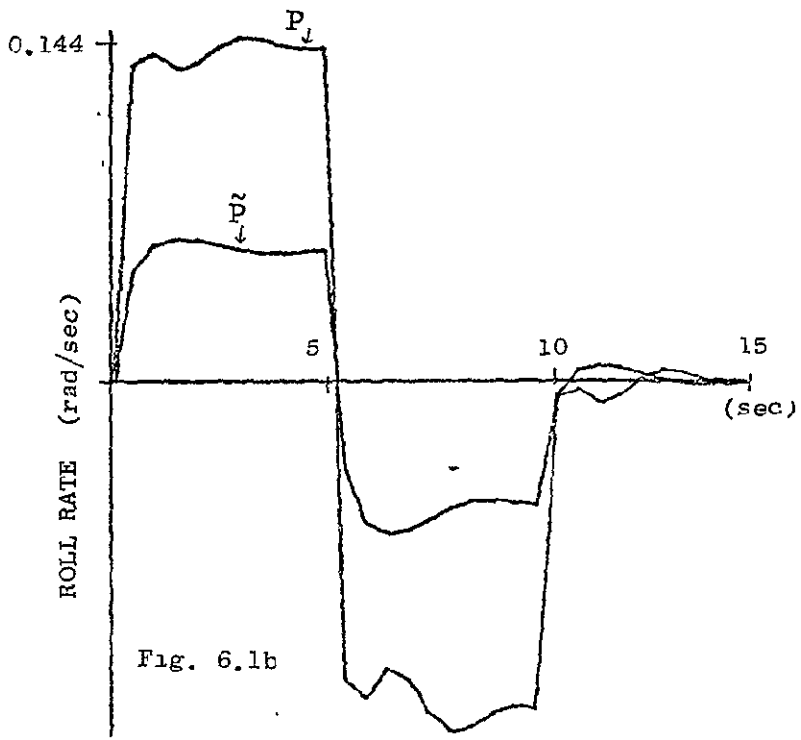

Fig. 6.1b

FIG. 6.1 RESPONSE OF THE FULL STATE ESTIMATOR TO A CONTROL INPUT.

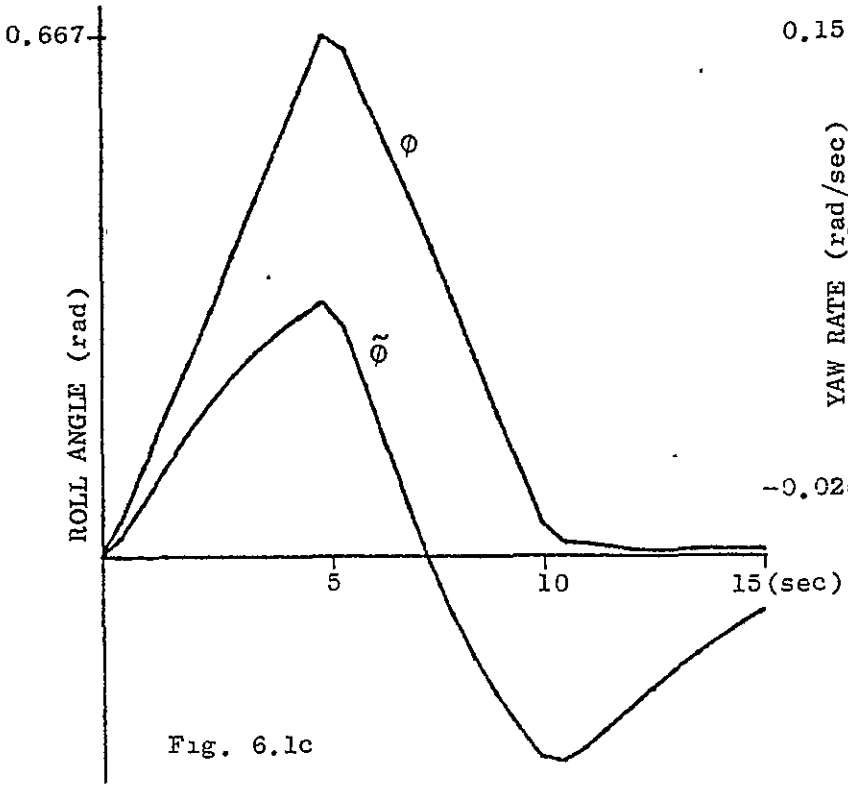

Fig. 6.1c

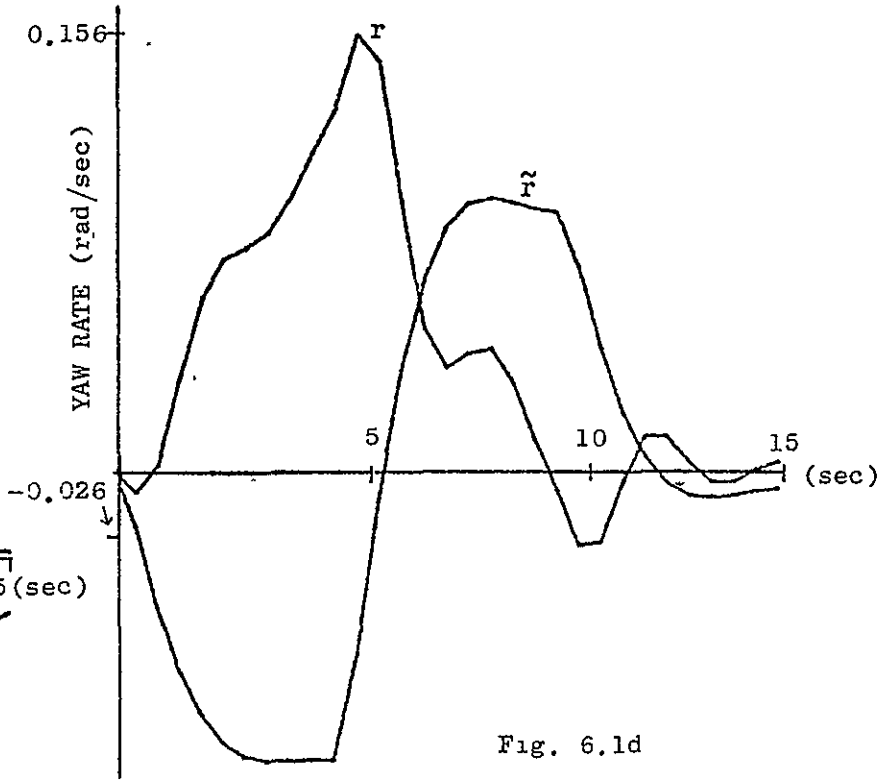

Fig. 6.1d

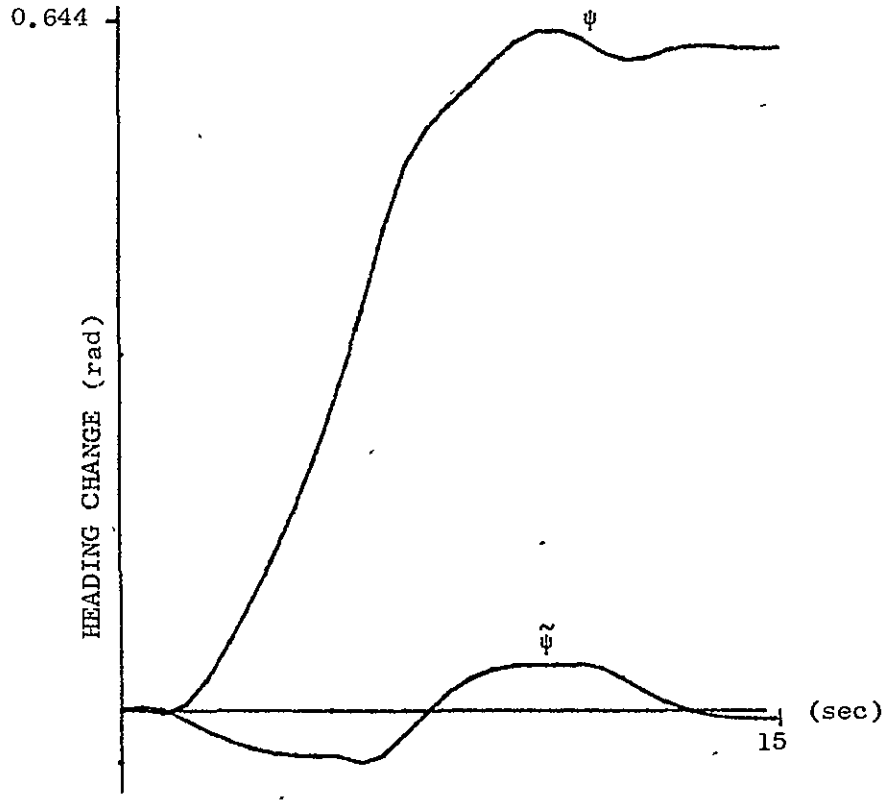

Fig. 6.1e

Kinematic Observer

An alternative mechanization is one in which an accelerometer is used as input to a kinematic equation, and these equations are used in place of the dynamic state equations. When this is done, the measured value itself is treated as an input, and hence is known just as the control inputs are assumed measured and therefore known in the case of the dynamic equations. There are certain combinations of linear and angular accelerometers that can be used as inputs rather than measurements that will simplify the mechanization and more importantly, reduce sensitivity to modeling errors.

This set of possible mechanizations assumed that the magnetometer is used to generate both heading and roll angles (with knowledge of pitch angle from the longitudinal estimator, and the dip angle of the earth's magnetic field). In addition, there are a maximum of three measurements: a_y, lateral acceleration, α_x, roll angular acceleration, and α_y, yaw angular acceleration. Given the assumption that all mechanizations will include the linear accelerometer measurement of a_y due to the lowest instrument cost, there are four possible mechanizations, labeled "Types I through IV."

It should be noted that extracting both heading and roll information from the magnetometer would require either some form of vertical reference based on specific force measurements which are filtered to get rid of acceleration (employing a gyro) or a processing scheme that would attempt to resolve ambiguities in heading as the aircraft passed through magnetic north or south. The following estimator mechanizations were studied to examine the results of using accelerometer signals as inputs and of not using control surface deflections in the estimator.

Type I Estimator

$$\left.\begin{aligned}
\dot{\hat{v}} &= -U_o\hat{r} + W_o\hat{p} + (g\cos\theta)\hat{\phi} + a_y \\
\dot{\hat{p}} &= \alpha_x \\
\dot{\hat{r}} &= \alpha_y \\
\dot{\hat{\phi}} &= \hat{p} + (\tan\theta)\hat{r} \\
\dot{\hat{\psi}} &= (\sec\theta)\hat{r}
\end{aligned}\right\} + K \begin{bmatrix} z_1 - \hat{z}_1 \\ \\ z_2 - \hat{z}_2 \end{bmatrix} \qquad (6.2)$$

where $z_1 = \phi_{measured}$, and $z_2 = \psi_{measured}$, and a_y, α_x, α_z are accelerometer inputs. Note that no control input is required since its effects are measured by the accelerometers. In this set of equations, v is not observable, a drawback for an autopilot, but not for a display. Ignoring the $\dot{\hat{v}}$ equation, the system can be mechanized as two decoupled second-order systems in (ϕ,p) with measurement of ϕ and input α_x, and (ψ,r) with measurement ψ and input α_y. The disadvantage here is that two relatively expensive angular accelerometers are needed. If use of either one (or both) of the angular accelerometers is to be avoided, an equation with aerodynamic terms must be substituted for it. The mechanization without the angular accelerometer in yaw is labeled Type II.

Type II Estimator

Here, aerodynamic terms are used instead of α_z, thus reducing the inputs to a_y, α_x

$$\left.\begin{aligned}
\dot{\hat{v}} &= -U_o\hat{r} + W_o\hat{p} + (g\cos\theta)\hat{\phi} + a_y \\
\dot{\hat{p}} &= \alpha_x \\
\dot{\hat{r}} &= N_v\hat{v} + N_p\hat{p} + N_r\hat{r} + N_{\delta a}\delta a + N_{\delta r}\delta_r \\
\dot{\hat{\phi}} &= \hat{p} + (\tan\theta)\hat{r} \\
\dot{\hat{\psi}} &= (\sec\theta)\hat{r}
\end{aligned}\right\} + K\begin{bmatrix} z_1 - \hat{z}_1 \\ \\ z_2 - \hat{z}_2 \end{bmatrix} \qquad (6.3)$$

Note here that the $\dot{r}$ equation has the same terms as in equation (6.1) including control terms. There will be none of the large errors caused by

mismodeling of G, there being no state derivative measurements (the terms a_y and α_x are treated as inputs here). In fact, it has proved possible to ignore the effect of control entirely, even for control-forced behavior, if the gains are chosen appropriately. If the gains chosen are

$$K = \begin{bmatrix} 0 & 48000. \\ 200. & 0 \\ 0 & 371. \\ 20. & 0 \\ 0 & 29. \end{bmatrix} \tag{6.4}$$

then the roots of the estimator equation are: -4.08, -12.9 ± 11.2, -10.0 ±10.0 sec^{-1}. While there was no need for the roots to be so fast, this was done to simulate the effect of using no control input in the observer. Note that these roots were obtained with only five nonzero gains. Figures 6.2a-e show the results of the same type of simulation done for the aerodynamic estimator.† There was, however, an assumed difference of 50 ft/sec between the actual speed of the aircraft, and that used to calculate N_v, N_p, and N_r, the only speed dependent terms in the observer ($N_{\delta a}\delta_a$ and $N_{\delta r}\delta_r$ were assumed zero, and thus there would be no need to instrument the ailerons and rudder). Note that the only objectionable error is that in the lateral velocity, which is approximately 20-30% of the magnitude of the velocity itself. Simulations involving a step in rudder yielded equally good results for yaw and roll angles and rates, but worse errors in lateral velocity. These approached the magnitude of the lateral velocity for the

† Comparable to Figures 6.1a-e.

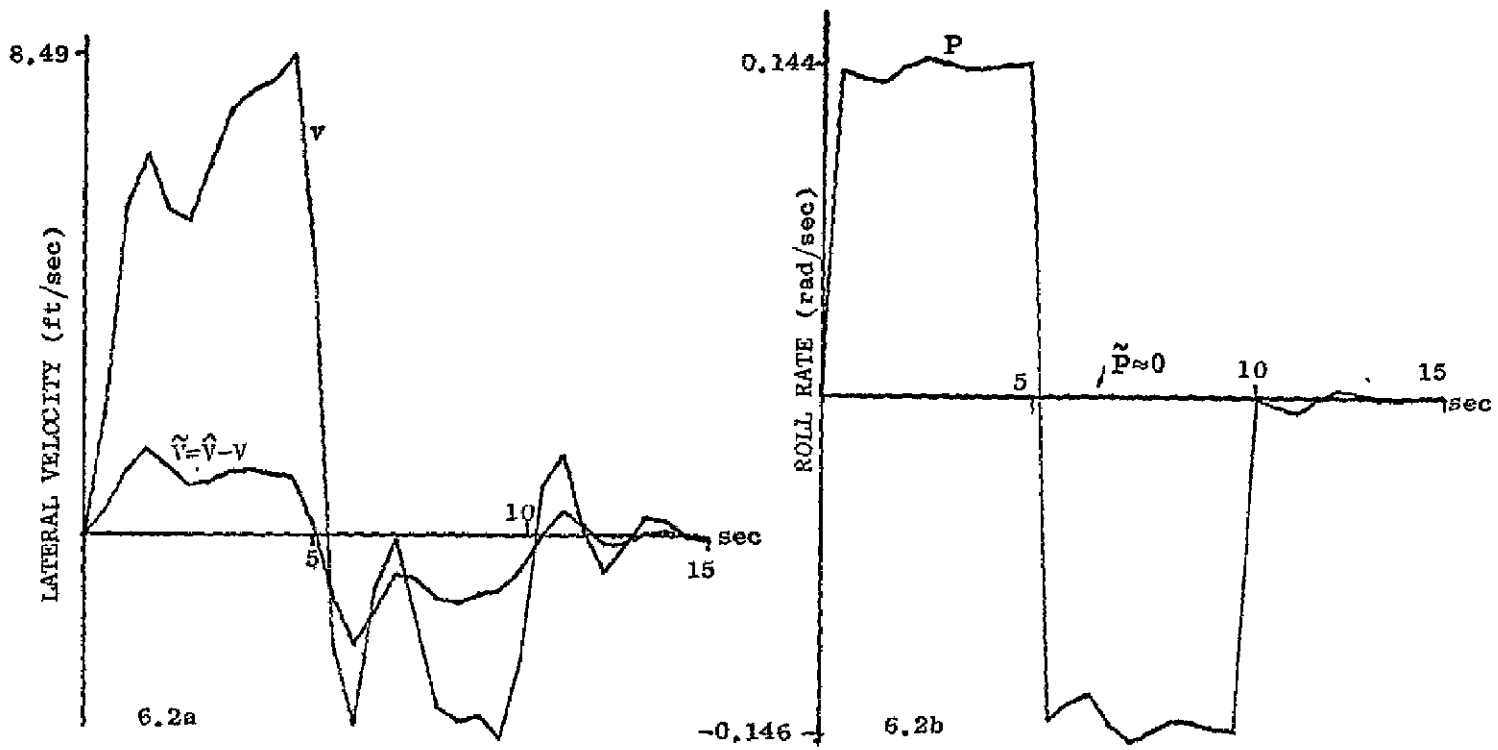

Fig. 6.2a, b RESPONSE OF THE TYPE II ESTIMATOR TO A CONTROL INPUT

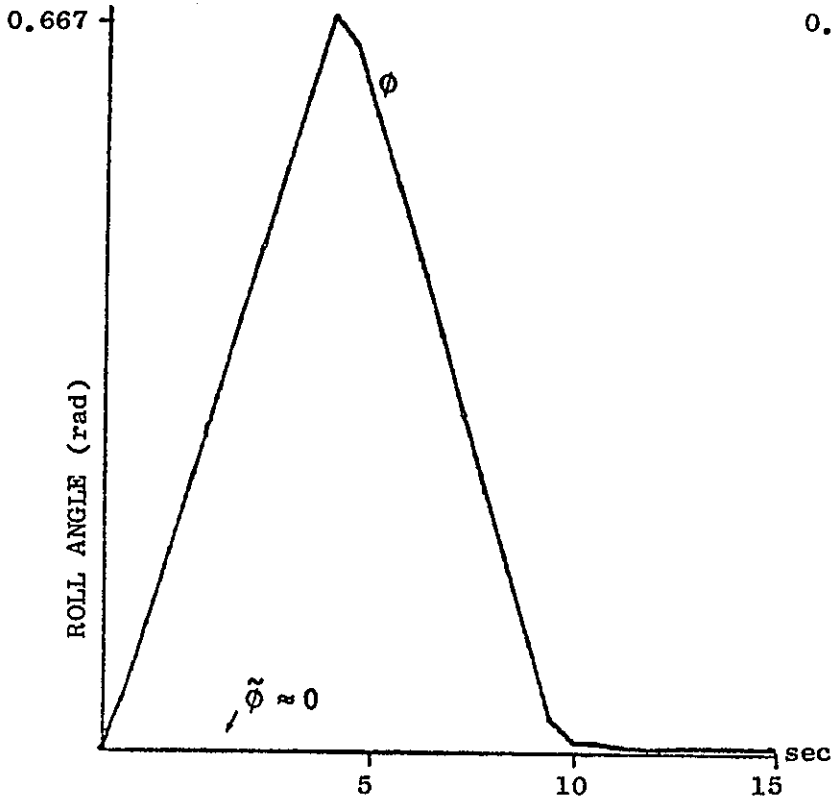

Fig. 6.2c

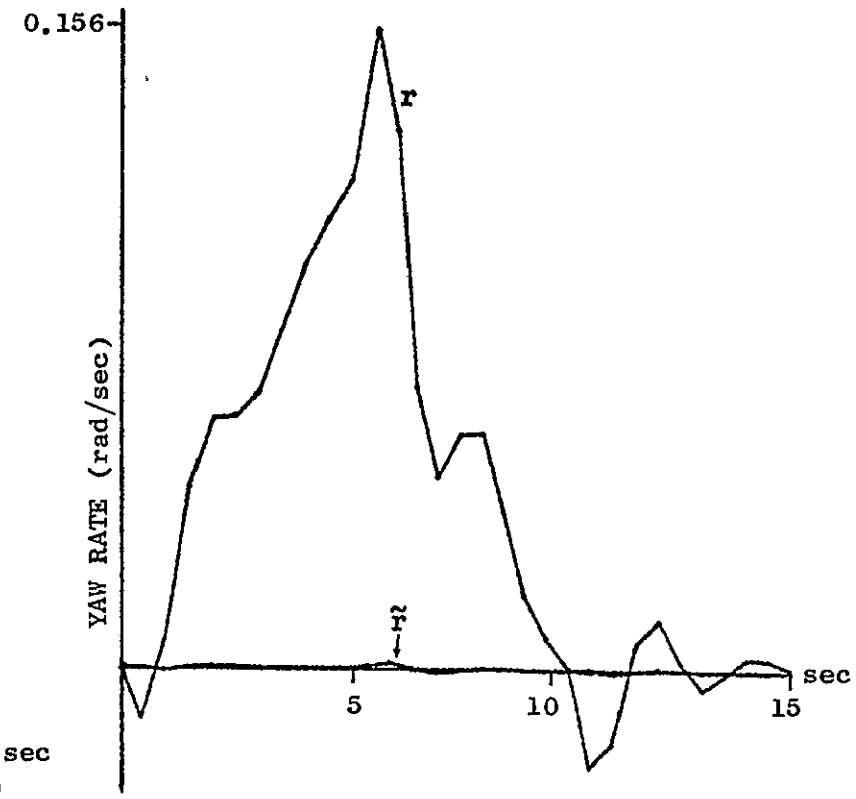

Fig. 6.2d

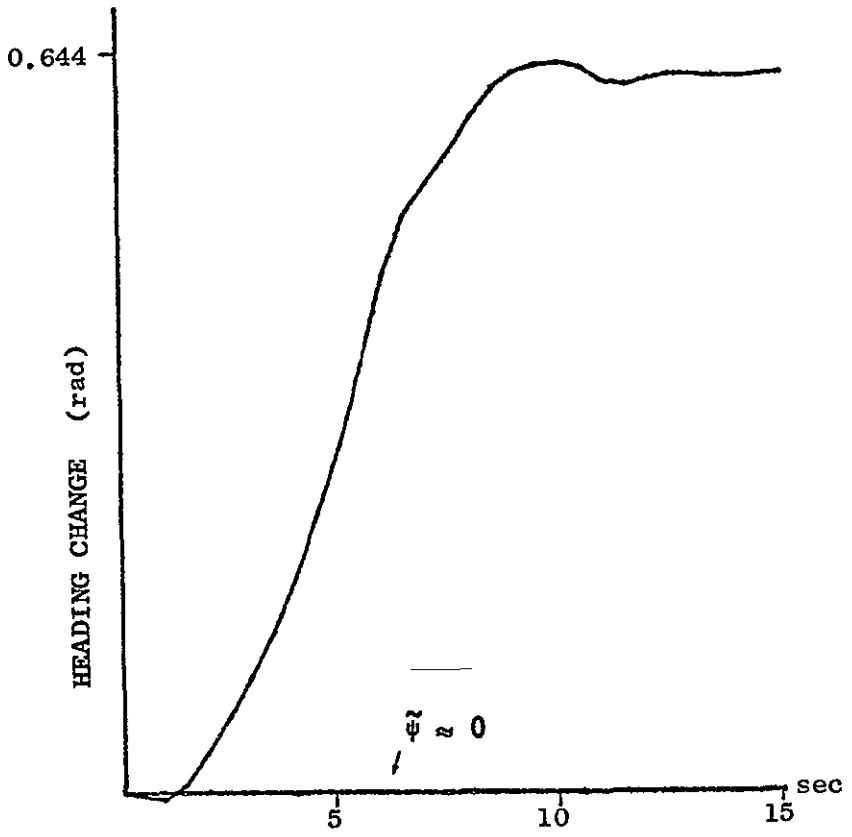

Fig. 6.2e

same assumed 50 ft/sec speed error. These errors can be reduced with gain scheduling or with the inclusion of the control terms.

Type III Estimator

Here, aerodynamic terms are used to replace α_x .

$$\left.\begin{aligned}
\dot{\hat{v}} &= U_o\hat{r} + W_o\hat{p} + (g\cos\theta)\hat{\phi} + a_y \\
\dot{\hat{p}} &= L_v\hat{v} + L_p\hat{p} + L_r\hat{r} + L_{a}\delta_a + L_{r}\delta_r \\
\dot{\hat{r}} &= \alpha_z \\
\dot{\hat{\phi}} &= \hat{p} + (\tan\theta)\hat{r} \\
\dot{\hat{\psi}} &= (\sec\theta)\hat{r}
\end{aligned}\right\} + K\begin{bmatrix} z_1 - \hat{z}_1 \\ \\ z_2 - \hat{z}_2 \end{bmatrix} \qquad (6.5)$$

The Type III estimator, employing the angular accelerometer for yaw instead of roll, did not perform as well as the Type II estimator did for lateral velocity (without inclusion of control terms). It did as well for the other states.

Type IV Estimator

Here aerodynamic terms are used to replace α_x and α_z:

$$\left.\begin{aligned}
\dot{\hat{v}} &= U_o\hat{r} + W_o\hat{p} + (g\cos\theta)\hat{\phi} + a_y \\
\dot{\hat{p}} &= L_v\hat{v} + L_p\hat{p} + L_r\hat{r} + L_{a}\delta_a + L_{r}\delta_r \\
\dot{\hat{r}} &= N_v\hat{v} + N_p\hat{p} + N_r\hat{r} + N_{a}\delta_a + N_{r}\delta_r \\
\dot{\hat{\phi}} &= \hat{p} + (\tan\theta)\hat{r} \\
\dot{\hat{\psi}} &= (\sec\theta)\hat{r}
\end{aligned}\right\} + K\begin{bmatrix} z_1 - \hat{z}_1 \\ \\ z_2 - \hat{z}_2 \end{bmatrix} \qquad (6.6)$$

The Type IV estimator, with only a linear accelerometer, is very close in form to the purely aerodynamic estimator, although there is no measurement of state derivatives. Its simulation response suffered severely from lack of control inputs. This is intuitively reasonable since there are no angular accelerometers to measure the immediate direct effect of the control. Were such a mechanization to be used, both lateral control surfaces would have to be instrumented.

Vector Mechanization

It is convenient for conceptualizing and checkout to keep as many modes separated as possible. On the other hand, the evaluation of the interaction between lateral and longitudinal behavior is best done with the integrated equations. For example, pitch influences the magnetometer readings, B, and hence heading information needed in the lateral equations. A set of combined equations for the orientation is derived for any two known spatially fixed noncolinear vectors. Their time derivatives in space is zero so in body axes we get

$$\overset{b}{\hat{B}} = -\hat{\omega}^{b} \times \hat{B} + K_{B}(B^{m} - \hat{B}) \tag{6.7}$$

$$\overset{b}{\hat{g}} = -\hat{\omega}^{b} \times \hat{g} + K_{g}(-f^{m} - \hat{g}) + K_{gB}(B^{m} - \hat{B}) \tag{6.8}$$

and

$$\overset{b}{\hat{\omega}} = \alpha^{m} + K_{\omega B}(B^{m} - \hat{B}) + K_{\omega g}(-f^{m} - \hat{g}) \tag{6.9}$$

where K_{gB} and $K_{\omega g}$ may be zero and b implies differentiation or coordinates with respect to the body. (Other estimator feedback combinations may prove to be more effective.)

These equations could be simplified slightly by the direct use of a measured ω from a rate gyro set. Similarly, we can write the vector form for the acceleration but using the specific force as an input

$$\overset{b}{\hat{V}} = -\hat{\omega}^{b} \times \hat{V} + f^{m} + \hat{g} + K_{v}(U^{m} - \hat{U}) + K_{vB}(B^{m} - \hat{B}) \tag{6.10}$$

where again, K_{vB} may be zero.

Finally, the altitude equation using a local frame ℓ for vertical velocity component

$$\dot{\hat{h}} = -\hat{V}_{3\ell} + K_h(h^m - \hat{h}) \quad . \tag{6.11}$$

Although all terms of the direction cosine matrix are not needed

$$\hat{C}_{b/\ell} = [\hat{B}_b, \ \hat{g}_b, \ (\hat{B}_b \times \hat{g}_b)] \cdot \underbrace{[B_\ell, \ g_\ell, \ (B_\ell \times g_\ell)]^{-1}}_{\text{known}} \tag{6.12}$$

from which the necessary terms for

$$\hat{V}_{3\ell} = [\hat{C}_{11}, \ \hat{C}_{21}, \ \hat{C}_{31}] \begin{bmatrix} \hat{V}_{1b} \\ \hat{V}_{2b} \\ \hat{V}_{3b} \end{bmatrix} \tag{6.13}$$

can be expressed in terms of $\hat{B}_b$ and $\hat{g}_b$.

Using the same relationship, the indication of pitch and roll altitude will be the direction cosine elements

$$\text{pitch} = -\hat{1}b \cdot \hat{3}\ell = -\hat{C}_{13} \tag{6.14}$$

$$\text{roll} = +\hat{2}b \cdot \hat{3}\ell = \hat{C}_{23} \tag{6.15}$$

which can each be expressed more simply in terms of $\hat{B}_b$ and $\hat{g}_b$.

Since the local frame will be defined as $\hat{1}\ell$ = magnetic north only the dip angle need be estimated in flight (or set occasionally).

This mechanization has not been simulated in detail. Preliminary evaluation suggests that the gains K_B should be appropriate for filtering electronic noise ≤ 1 sec whereas the K_g should be comparable to the evection gains for an artificial horizon producing a few hundred second time constant and having a cutout for large maneuvers or at least

a saturation level for the whole term involving K_g. The other gains follow a pattern discussed previously in Ch. V.

VII.

CONCLUSIONS AND RECOMMENDATIONS

Modeling aircraft dynamics can give more flexibility in the choice of sensors needed to measure adequately the states of an aircraft. The models make it possible to infer states with indirect measurement. We have shown that an instrument set composed of linear and angular accelerometers, mangetometer, and pressure transducers is adequate. This complement of instruments should be able to take advantage of the emerging state of silicon technology spawned by the semiconductor market which promises great reliability and low cost. The use of the aircraft dynamic equations in an estimator has been shown to be feasible, but errors are introduced which depend on disturbing forces and torques (due to winds) and in some axes, it is important to include control inputs. Purely kinematic equations are not as sensitive to modeling omissions but there are questions of observability. Thus we have been led to a combination of kinematic and dynamic equation relations which minimizes the dependence on wind and disturbance modeling, and do not require control inputs. This is true for both longitudinal and lateral equations.

In addition, states representing orientation, velocity, and altitude in an integrated vector format have been considered but not evaluated in detail. An estimator was designed this way which has the appeal of having a close analogy with an artificial horizon. On the average, the specific force is gravity if the velocity is to be bounded. The strong dependence on the angular velocity in these equations suggest that an alternate configuration of sensors should include rate gyros.

Thus it is concluded that the combination of three accelerometers, two angular accelerometers, a three-axis magnetometer, absolute pressure and pitot pressure are an adequate set of sensors for the estimation of orientation, altitude, and velocity states. Reasonable performance requirements are required and can be met by existing instruments though not in

all cases by the smallest or least expensive as originally hoped. Since the new technology is expected to continue to develop, it is recommended that the feasibility of this approach be established with available sensors on the expectation that reductions in cost and improvements in reliability will follow soon and may be available by the time a flight evaluation is under way. Silicon technology is adequate for pitot pressure now but development is still needed for barometric altitude measurement. Silicon technology accelerometers may be acceptable but an experimental evaluation must be completed with instrument tests before a decision can be reached. Feedback type fluxgate magnetometers are adequate but non-feedback types must be tested to determine if their characteristics are stable enough for online modeling.

It is recommended that the candidate instrument package flown include three axes of rate gyros angular accelerometers, linear specific force, magnetic field, and the two pressures. In this way extra measurements may be included or not in the off-line evaluation.

APPENDIX A

This Appendix includes detailed Tables, mentioned in Chapter IV, for the following:

LINEAR ACCELEROMETERS (4 pages)

ANGULAR ACCELEROMETERS

ANGULAR RATE SENSORS (2 pages)

MAGNETOMETERS

ABSOLUTE PRESSURE TRANSDUCERS (4 pages)

DIFFERENTIAL PRESSURE TRANSDUCERS (airspeed) (3 pages)

LINEAR DISPLACEMENT TRANSDUCERS (3 pages)

Mfr. & Life	Model	Range	Type	dc Sensitivity	f_m and Damping	Non-linearity	Thermal Sens. Shift	Thermal Bias Shift	Zero Offset	Transverse Sens'vy	Noise	Qty Price	Size or Weight
Entran	EG-D240 -10	± 10g	Piezoresistive C. beam	10 mV/g at 10V ex.	500 Hz 0.005	2%FS	10-16% per 100°F	5 g per 100°F	±10g	5% max		1-4 @ $120; 1000 $50.	4 gm
Entran	EGC-240-D5	±5g	"	25 mV/g at 15V ex.	370 Hz 0.7	1% of reading	±2.5% per 100°F	±2.5% FS per 100°F	±0.6g	3% max		1-9 @ $270; 25-49 $230.	4 gm
Kistler-Morse	201-020	±20g	Piezoresistive	30 mV/g at 10V ex.	150 Hz	0.5% inc. hyst and thr.		±2% FS per 100°F		0.1%	1μV per V	1, $160; 25, $120.	50 gm
Genisco 10^6 cycles	2386	±5g	Pot.	1V/g @ 10V ex.	24 Hz 1.8-0.25 -10-185°F	±1% FS static error	±2%FS Combined static error -10°F to + 185°F					1@$412. 150 up $337.	3"×1⅓" × 1⅛"
Genisco 10^4 hours	2388	±5g	Variable Reluctance	ac phase sensitv.	30 Hz 0.5-0.9 -65-185°F	±1% FS static error	± 1.5% FS combined static error -65°F to + 185°F					1@$563. 150 up $457.	2" × 2" × 2½"
C.J. Enterprises	A18	±5g	"	"	170 Hz 0.6-0.7 @ 25°C	±0.5% linearity; ±0.25% hysteresis.	2%/100°F	1%/100°F	0.5g	0.01 g/g		$575	3 oz.
Timex	APM-000	±2.5g	Differential xfmr.	"	25 Hz 0.4-0.9 -65-185°F	±0.1%FS @±1.25g; ±2% FS @ ± 2.5g	4% per 100°F	0.12% per 100°F	1.25×10^{-3}g @ 20°C				3 oz
Kulite	GAD-813 -10	±10g	semicon-strain gage	12 mV/g @ 10V ex	450 Hz 0.5 @ 25°C	±1% FS static error	2% per 100°F	0.33g 80°F to 180°F	N.S.	5% max.		$275.	1¾ oz
Teledyne	FP 1	±15g	force rebalance			$20\mu g/g^2$	0.1 % per 100°F	1.5×10^{-3}g per 100°F	10^{-5}g	10^{-5}g/g^2			15 gm
G.E.	LB-5	±20g	"	100mV/g	140 Hz 0.4-0.6	0.05% FS	operating range -54°C to 71°C		2×10^{-5}g threshold.		vib. cap. .06g^2 per Hz	Sold only with systems	2.50 oz

A-1

LINEAR ACCELEROMETERS

Mfr. & Date	Model	Range	Type	dc Sensitivity	f_n and Damping	Non-linearity	Thermal Sens. Shift	Thermal Bias Shift	Zero Offset	Trans-verse Sens'v	Noise	Qty Price	Size or Weight
Sundstrand	303GA5	±5 g	Non-pendulous Servo	1 v/g	650 Hz ±5% to 390 Hz	±0.05% FS	1% per 100°F	0.05 g per 100°F	±0.1 g	None to actual sen. axis	5 mV RMS	$595	3.3 oz
Ferranti	FA. 21	±20 g	Pendulous Servo current	5 ma/g ± 0.01%	N.S. electronic or viscous	±0.05% accuracy	0.56% per 100°F	0.4×10^{-2} g per 100°F	3×10^{-4} g				80 gm
Sanders > 1000 hrs	30 - 5	±5 g	Pendulous differen-tial xfmr.	AC 1.12V rms per g	33 Hz 0.5 fluid	±0.2% FS to ±2.5 g ±3% FS to ±5 g	4% per 100°F		0.05% FS				4.5 oz
Setra	113 triaxial	±25 g	Seismic disc cap. p.o.	60 mV/g	800 Hz 0.7 gas squeeze film	±1% FS	±2% FS per 100°F	±2% FS per 100°F	±50 mV at 77°F	0.01g/g	<2 mV rms	1 - 4 $142 per axis ($425)	4 oz
Larson	Cal	±5 g	Pendulous Servo	1 V/g	120 Hz 0.4 to 1 Electro magnetic	±1% FS Lin, HYST, Repeat-ability	±3% per 100°F		±1% FS	0.005g/g		Small $129	1 oz
Bell and Howell	4-205-0001	±1.0 g, ±2 5 g, or ±5 g	Unbonded strain gage	40 mV. full range 5 V ex.	"High" 0.7 ± 0.1 @ 77°F	±0.75% of full range lin. + hyst.	temp. compensated -65°F to +250°F			"Low"		Small $415	4.5 oz
West Coast Research	703	0.5, 1, 2, 5, or 10 g	Bonded strain gage	1mV/V FS, 10mV/V FS, 1V FS, or 5 V FS	20 - 500 Hz 0.4	% FS 0.5 lin 0.5 hyst 0.25 re-peat.	1% per 100°F	1% per 100°F		1%		1 $295 to $340 1000 $177 to $204	3 to 7 oz

Mfr. & Life	Model	Range	Type	dc Sensitivity	f_m and Damping	Non-linearity	Thermal Sens. Shift	Thermal Bias Shift	Zero Offset	Transverse Sens'v	Noise	Qty Price	Size or Weight
Humphrey $2x10^7$ cycles 1 axis or 3 axis units avail.	LA 45 LA 67 LA 88 LA 83	0.25 g to 200 g combo. ok	Spring flex with pot	pot " " ±2.5 V	dry gas damping	±1.5% accuracy	wire wound pot cond. plastic pot wire wound pot wire wound pots		0.8% resolution on pots	N.S N.S low N.S	1 axis " " 3 axis	1 - 5 $255 $210 $440 $990	1 oz
Bourns. 10^7 cycles	633	±5 g	Spring mass suspension cond. plastic pot	1 V/g 10 V ex.	30 Hz 0.7±0.3	Static includes temp.	error band ±1.5% of FS		Incl. in static error B	0.06 g/g	Vib. Sens. ±1.5% except at res.	1 $150 1000 $85.15	7 oz
Gould Statham	A6-5-350 or A73TC	±5 g ±4 g	Unbonded strain gage	4 mV/V Full scale	75 Hz 0.7±0.1 300 Hz	±1% FS includes hysteresis	Specified in Model A at 0.01%/°F	73 TC $495.00 0.01%/°F		0.02g/g 0.01g/g		1 - 3 $465 1 - 3 $495	1.3 oz 3 oz
Schaevitz	LSBP-5	±5 g	Force Rebalance Servo	±5V±0.2% Full range	125 Hz 0.55 to 0.75	±0.05% Full scale	1% per 100°F	Operating range -40°F to +200°F	< 0.1% Full scale	±0.002 g/g	5 mV rms max random	1 - 2 $539 100-199 $410	3 oz
Donner	4383	±20 g to ±40 g	Pendulous Servo	±4 V Full range	150 Hz 1.2±0.2 @ 20°C	12 mg max.	0.02% of value per °C	0.3 mg per °C	20 mg max	0.002 g/g	2 mV nms wide band	1 - 10 $400 1000 $300	85 gm
Bell Aerospace	Model 9		Inertial grade										
Signetics	Under development	±20 g	Solid State	±10 V Full range	700 Hz 0.03 squeeze film	±1% Full scale		0.3% FS per °C w/o temp control	0.003% FS/°C zero shift w. temp. con.	0.01g/g			28 pin D.I.P. ceramic

BEST SELLERS

FROM NATIONAL TECHNICAL INFORMATION SERVICE

NTIS

Development of Pre-Mining and Reclamation Plan Rationale for Surface Coal Mines
PB-258 041/SET/ PAT 590 p PC$22 50/MF$7.00

Manual of Respiratory Protection Against Airborne Radioactive Materials
PB-258 052/PAT 147 p PC$6 00/MF$3 00

Design and Construction of a Residential Solar Heating and Cooling System
PB-237 042/ PAT 233 p PC$8.00/MF$3.00

1976 Energy Fact Book
ADA-029 331/ PAT 195 p PC$12 50/MF$12 50

Impacts of Construction Activities in Wetlands of the United States
PB-256 674/ PAT 426 p PC$11 75/MF$3 00

Standardized Development of Computer Software. Part I: Methods
N76-30-849/ PAT 389 p PC$10 75/MF$3 00

A Methodology for Producing Reliable Software, Volume I
N76-29-945/ PAT 228 p PC$8 00/MF$3.00

Flow and Gas Sampling Manual
PB-258 080/ PAT 102 p PC$5 50/MF$3 00

Solar Heating and Cooling in Buildings: Methods of Economic Evaluation
COM-75-11070/ PAT 48 p PC$4 00/MF$3 00

Data Base Directions The Next Steps
PB-258 103/ PAT 177 p PC$7 50/MF$3 00

Comparative Study of Various Text Editors and Formatting Systems
ADA-029 050/ PAT 93 p PC Not Available/MF$3 00

Explaining Energy: A Manual of Non-Style for the Energy Outsider Who Wants In
LBL-4458/ PAT 78 p PC$4.50/MF$3 00

A Survey of State Legislation Relating to Solar Energy
PB-258 235/ PAT 166 p PC$6 75/MF$3 00

Cost Estimating Handbook for Transfer, Shredding and Sanitary Landfilling of Solid Waste
PB-256 444/ PAT 85 p PC$5 00/MF$3 00

Coal Liquefaction Design Practices Manual
PB-257 541/ PAT 372 p PC$10.50/MF$3 00

HOW TO ORDER

When you indicate the method of payment, please note if a purchase order is not accompanied by payment, you will be billed an additional $5 00 *ship and bill* charge And please include the card expiration date when using American Express

Normal delivery time takes three to five weeks It is vital that you order by number or your order will be manually filled, insuring a delay You can opt for *airmail delivery* for $2 00 North American continent, $3 00 outside North American continent charge per item Just check the *Airmail Service* box If you're really pressed for time, call the NTIS Rush Handling Service (703)557-4700 For a $10 00 charge per item, your order will be airmailed within 48 hours Or, you can pick up your order in the Washington Information Center & Bookstore or at our Springfield Operations Center within 24 hours for a $6 00 per item charge

You may also place your order by telephone or if you have an NTIS Deposit Account or an American Express card order through TELEX The order desk number is (703) 557-4650 and the TELEX number is 89-9405.

Thank you for your interest in NTIS. We appreciate your order

METHOD OF PAYMENT

- ☐ Charge my NTIS deposit account no. _____
- ☐ Purchase order no. _____
- ☐ Check enclosed for $_____
- ☐ Bill me. Add $5.00 per order and sign below. (Not available outside North American continent.)
- ☐ Charge to my American Express Card account number

Card expiration date_____

Signature _____

☐ Airmail Services requested

NAME_____

ADDRESS_____

CITY STATE ZIP_____

Item Number	Quantity		Unit Price*	Total Price*
	Paper Copy (PC)	Microfiche (MF)		

All prices subject to change The prices above are accurate as of 4/77

Foreign Prices on Request

Sub Total	
Additional Charge	
Enter Grand Total	

Clip and mail to

NTIS

National Technical Information Service
U.S DEPARTMENT OF COMMERCE
Springfield, Va 22161
(703) 557-4650 TELEX 89-9405

Mfr. & Life	Model	Range	Type	dc Sensitivity	f_m and Damping	Non-linearity	Thermal Sens. Shift	Thermal Bias Shift	Zero Offset	Transverse Sens'v	Noise	Qty Price	Size or Weight
Conrac	24185	±1 g to ±20 g	Spring restrained seismic mass. pot	±5 V Full range 10 V ex.	8 to 41 Hz 0.3 min.	±1% FS with 0.2g 60Hz vibration	±1% additional error over -65°F to 200°F		1 to 2% @ 25°C	0.005g/g			6 oz

Manufact'r and Life	Model	Range	Type	dc Sensitivity	f_m and Damping	Non-linearity	Thermal Sens. Shift	Linear Acceler-ation Sens.	Thres-hold	x Axis Sens.	Noise	Qty. Price	Size or Weight
Donner	4590	±0.1 to 10	Liquid rotor sensor	±5 V full range	30 Hz @ 1 r/s^2	0.1% of full range	3% per 100°F	0.02% per g	0.001% full range	0.01r/s^2 per r/s^2	0.07% full range	1-10 $3000 100-500 $2500	3 lbs
Donner	4591	±10-200 rad/sec^2	Liquid rotor sensor	±2.5 V full range	To 150 Hz 0.6±0.2 @ 72°F	0.1% of full range	3% per 100°F	5 mV per g	0.001% full range	3 mV per rad/sec^2	10mV rms	1-10 $3000 100-500 $2500	8.5 oz
Schaevitz	ASBP-5 -10 -15	5 r/s^2 10 r/s^2 15 r/s^2	Torque rebalance Servo	±5V±2% full range	12 to 24 Hz 0.55 to 0.75	±0.1% full scale	1% per 100°F	0.1 r/s^2 per g	< 0.1% zero offset		5 mV rms	1-2 $664 100-199 $504	3 oz
Donner	4577	100r/s^2	torque re-balance servo	0.025Vdc per r/s^2						0.004 V/r/s^2	10mV	500 $400	5 oz

ANGULAR ACCELEROMETERS

Manufact'r and Life	Model	Range	Type	dc Sensitivity	f_n and Damping	Non-linearity	Thermal Sens. Shift	Linear Acceleration Sens.	Threshold	x Axis Sens.	Ther. Bias Shift or Noise	Qty. Price	Size or Weight
Donner MTBF > 60,000 hrs	8160	±5°/sec to ±100°/sec	Liquid rotor with integrator	±5 Vdc full scale	f_{n1} 0.007 Hz f_{n2} 30 Hz 0.6±0.2	< 1% full scale	< 5% per 100°F	*Note +2 slope below 0.007Hz	<0.001% full scale	0.005 °/sec per °/sec	1.5% per 100°F	1-20 $1455 100 $1185 500 $995	< 10 oz
Humphrey 3 units cont. op for 6 yrs.	RT03-0108-1	±200° per second	Electro fluidic 1 axis	±2.5 Vdc ±10%	50 Hz	±2°/sec	5% -40°F to +170°F				10% per 100°F	1-5 $935	2.6" D 0.4" L
Humphrey 3 units cont. op for 6 yrs.	AT10-0102-1		Electro fluidic 2 axis				5% -40°F to +170°F		2% available on special order add $50 to 100		10% per 100°F	1-5 $1675	2.6" D 4" L
Humphrey 3 units cont. op for 6 yrs.	RT02-0201-1	Pitch ±60°/s Roll ±360°/s Yaw ±60°/s	Electro fluidic 3 axis	0 to + 5 Vdc	30 Hz to 80 Hz	±1%	5% -40°F to +170°F				10% per 100°F	1-5 $3500	3" x 4.6" x 3.7"
BAC, Ltd.	RG408 Dart	±20°/sec to ±300°/sec	2 axis									1-5 $3500	0.7" D 2.2" L
Honeywell	GG2500 LC02	±480°/sec	Magneto-hydro-dynamic with spin motor 2 axis	15mVrms per °/sec ±2%	100 Hz	0.1% FS		0.05 deg/sec/g	0.01 deg/sec	0.5% FS	150 mVrms @ 1kHz band width	1 $1000 w/o electronics	0.7" D 1.8" L 70 gm

ANGULAR RATE SENSORS

Manufact'r and Life	Model	Range	Type	dc Sensitivity	f_m and Damping	Non-linearity	Thermal Sens. Shift	Linear Acceler-ation Sens.	Thres-hold	x Axis Sens.	Noise	Qty. Price	Size or Weight
Honeywell cont.	"		"										
with electronic package for above	plus EG1030 AB03	±100°/sec		87mVdc per °/sec ±2%	-3 db @ 70 Hz	0.1% FS		0.05 deg/sec/g	0.01 deg/sec	0.5% FS	2mVrms @ null 145 mVrms @ FS	1 $200 *	1.05" x 2.27" x 1.9"

ANGULAR RATE SENSORS

*electronics only

Manufact'r	Model	# Axis	Type	Range	Axis Allign-ment	Scale Factor Accuracy	Bias Accuracy	Noise	Temp. Stabil-ity	(dc) Sensi-tivity	Qty. Price	Size or Weight	Linearity
Develco	9200C	3	Fluxgate	±600 mg	±1°	±1%	±1% FS	1 Gamma p-p @ 1Hz b.w.	0.4 mg /°C	2.5V per 600 mg	1-3 $600 to $700 1000 $360	6 oz	±0.5% FS
Superconduct-ing Technology	F203	3	Fluxgate	±600 mg	±1°	±1%	±1% FS	NS	0.4 mg /°C	2.5F per 600 mg	1-3 $850 1000 $450	3.5 oz	±0.5% FS
Schonstedt	SAM - 73C	3	Fluxgate	±6J0 mg	±1°	±1%	±0.4% FS	1 Gamma p-p @ 1Hz b.w.	0.14 mg/°C	2.5 V per 600 mg	1-10 $1650 1000 $600	5 oz	±0.4% FS
Infinetics	Friskem Mark-26	1	Fluxgate	±600 mg	NS	NS	NS	NS	NS	0.192 V per 600 mg	1-3 $44 1000-2000 $34	1" D 2.5" L	Reason-able
Spartan Electronics	RCI	1	Fluxgate	±1500 mg	NS	±2% FS	NS	0.4 nT p-p T = 60sec	NS	1.2 V per 600 mg	1-6 $1000 1000 $200	1.75" x 1.5" x 0.75"	1% FS
Schonstedt	RM62-?	2	* Similar to Mr. Upton		SAM 73 C 8/17/76	per Telicon					100 $550	1 lb	

MAGNETOMETERS

Mfr. & Life	Model	Range	Type	dc Sensitivity	*Static Error	Thermal Bias Shift	Thermal Sens. Shift	Error @ Sea Level ±50°FΔT	Time Constant	Initial Zero Balance	Long Term Stab.	Qty Price	Size or Weight
Setra	250	0 to 20 PSIA	Quartz capsule cap. p.o.	5 V FS	±0.06%	0.1% per 100°F	0.1% per 100°F	±35 feet	10 ms max			1 $975	9 oz
Hamiliton Standard	PT-020S -10	0 to 20 PSIA	Vibrating cylinder	Freq. prop. to pressure	±0.016%	0.38% per 100°F compensatable		±13 feet	Frequency is non-linear with pressure			1 $1380	6.4 oz
Rosemount	1241A	-1000 to 30,000 feet	metal capsule cap. p.o.	7.5 V per 30,000'	±0.25% reading +20'	0.75% of reading inc. +40 feet static error		±47 feet	Output is linear with altitude			1 $1155	24 oz
Senso-Metrics 3×10^6 cycles	SP 65 E	0 to 15 PSIA	Bonded strain gage	200 mV FS ±2%	±0.05%	0.5% per 100°F	0.5% per 100°F	±100 feet		2% FS max		1 $900	3 oz
Gould Statham	PA 824-15	0 to 15 PSIA	Beam diaphragm deposited strain gage	30 mV FS	±0.15%	0.5% per 100°F	0.5% per 100°F	±109 feet	0.05 ms	< 2% FS	0.05% FS	1 $1265	14 oz
Bell and Howell	CEC 1000	0 to 15 PSIA	Diaphragm deposited strain gain	30 mV FS	±0.25%	0.5% per 100°F	0.5% per 100°F	±123 feet		±2% FS		1 $450	5 oz
BLH Electronics	DV	0 to 20 PSIA		5 V FS	±0.3%	1% per 100°F	0.5% per 100°F	±178 feet	0.05 ms	Adjust		1 $420	17 oz
Bourns	200 - 438 - 1002	Zero to 35,000'	Diaphragm with potentio-meter	10 V FS	±1.5% FS voltage ratio	2.5% error per 100°F		±825 feet	Output is linear with altitude			1-10 $375	13 oz

ABSOLUTE PRESSURE TRANSDUCERS (ALTITUDE) * linearity, hysteresis, and repeatability page 1 of 4

Mfr. & Life	Model	Range	Type	dc Sensitivity	*Static Error	Thermal Bias Shift	Thermal Sens. Shift	Error @ Sea Level ±50°F△T	Time Constant	Initial Zero Balance	Long Term Stab.	Qty Price	Size or Weight
Schaevitz	PTD - 310A - 300W	0 to 18 PSIA	Diaphragm capsule with LVDT	2.5V FS	±1.1%	Operating temp. range -65°F to 200°F		±316 feet	1 ms	Adjust		1 - 2 $542	18 oz
Tyco	AB-15-ADE	0 to 15 PSIA	Diaphragm with semi-C. strain gage	100 mV FS ±1%	±0.5%	1% per 100°F	1% per 100°F	±245 feet				1 - 9 $285 100 $142	2 oz
Sundstrand	314 A	0 to 15 PSIA	Servo	0 to 10V FS	±0.057%	0.4% per 100°F	0.5% per 100°F	±92 feet	10 ms			1 $810	1.6" x 1.6" x 1.9"
Viatran	304		Diaphragm with strain gage	High level available	±0.15%					Adjust			
Consolidated Controls	415G40		Diaphragm bonded strain gage	30 mV FS	±0.25%	Thermal sens. < 0.5% FS per 100°F							3.5 oz
Gulton "Long"	3255	0 to 15 PSIA	Aneroid capsule with LVDT	0 to 5 V FS	±0.5%	Total error including temp. from -65°F to 250°F ±0.75%		± 175 ft.			out-standing		5 oz
Gulton	3261	0 to 15 PSIA	Aneroid capsule with pot	0 to 10V FS	±1% FS	Thermal sens. 1% per 100°F		±317 feet	0.3% represents 85' sea level	pot resolution at			2.5 oz
Daytronic	502	0 to 15 PSIA	Diaphragm with strain gage	30 mV FS.	±0.25%	0.5% per 100°F	0.5% per 100°F	±122 feet	0.3 ms	±2%		1 $295	2.5" D 3.5" L

ABSOLUTE PRESSURE TRANSDUCERS (ALTITUDE) * linearity, hysteresis, and repeatability page 2 of 4

Manufacturer and Line	Model	Range	Type	dc Sensitivity	*Static Error	Thermal Bias Shift	Thermal Sens. Shift	Error @ Sea Level ±50°FΔT	Time Constant	Initial Zero Balance	Long Term Stab.	Qty Price	Size or Weight
Honeywell	HG 280 Data Computer	AIR	Silicon pressure capsule	General purpose CPU employed				±14 feet	Sensor not sold separately		Altitude + airspeed + mach	1 $15 k	19 lb
Conrad 2 x 10^6 FS cycles min.	4715LC	0 to 15 PSIA	Silicon capsule and strain gage	50 mV ±2% FS	±0.3%	0.5% per 100°F	0.5% per 100°F	±131 feet		±1% FS		1 $700 500 $200	1.12" D 1.62" L
National	LX1602A	0 to 15 PSIA	Solid state silicon	+2.5 V to 12.5V FS	±2.1%	2.7% per 100°F	2.7% per 100°F	±800 feet		Inc. in static error	1000 hr inc. in static error	1 $80	5 gm
Cognition	CG4208	0 to 30 inches Hg	Solid state silicon	+1.5 V to +4.5V FS	±0.2%	Thermal effect 0.2% per 100°F		±140 feet		0.2%	0.3%	1 $150	2.5" x 1.5" x 0.75"
Kavlico	Gm5570-1	0 to 15 PSIA	26 Vac LVDT 400 Hz	2 Vac ±3% FS		1% per 100°F	1% per 100°F						2.25 L 1.25 D
Transducer Systems Inc.	ac/ac or dc/dc	0 to 15 PSIA	LVDT	100 mV rms or 2 Vdc FS	±2%	1% per 100°F		±1400 feet				1 $150 ac $250 dc	ac / dc: D 1½" / 2"; L 2" / 3½"
Robinson Halpern	155	0 to 15 PSIA	Capsule + LVDT + electronic circuit	0.5 to 5.5 Vdc FS	±0.5% FS	Compensated to ±2% FS of cal 0° to 180°F	75°F	±316 feet		Adj. on zero and span		1 $175	8 oz
Rosemount	1332A	0 to 15 PSIA	Capsule cap. p.o. electronics	0 to 5V FS	±0.11%	Combined effect per 100°F	thermal ±0.5%	±77 feet	5 ms max			1 $445	7 oz

ABSOULTE PRESSURE TRANSDUCERS (ALTITUDE) * linearity, hysteresis, and repeatability page 3 of 4

Manufac'r and Ltr	Model	Range	Type	dc Sensitivity	*Static Error	Thermal Bias Shift	Thermal Sens. Shift	Error @ Sea Level ±50°FΔT	Time Constant	Initial Zero Balance	Long Term Stab.	Qty Price	Size or Weight
Rosemount	542K1	High Level dc outputs	Altitude: airspeed: dynamic	h IAS pressure	-1000' to +40,000 feet ±(40' 125 to 550 knots ±(3.5 k or qc 0.75 to 17.16" Hg ±(0.5%			± 0.7% of rdg) 1% of rdg) FS + 1% of rdg)		-45°F to +160°F	0.2 mV/ft 10mV/k 0.4 V/"Hg	1 to 5 $2360 12-24 $2125	2 lb
I.C. Transducers, Inc. "long"	1750	0 - 15 PSIA	solid state silicon	50 mV F S.: minimum	±0.5% F.S.	combined effect ± 2% per 100°F	thermal	± 315'		±10mV		1-9 $135.	15 gm

ABSOLUTE PRESSURE TRANSDUCERS (ALTITUDE) * linearity, hysteresis, and repeatability page 4 of 4

Manufact'r and Life	Model	Range PSID (knots)	Type	dc Sensitivity	*Static Error PSID	Thermal Bias Shift	Thermal Sens. Shift	Over Range PSID (knots)	Initial zero Balance	Over Pressure		Qty Price	Size or Weight
Sensotec	TJE	2 (285)	Bonded Strain Gage	20 mV FS	±0.1%	0.25% per 100°F	0.25% per 100°F	3 (342)				1 $524	2.5" L 2.25" D
Sensotec	Z	2 (285)	Bonded Strain Gage	20 mV FS	±0.3%	0.5% per 100°F	0.5% per 100°F	3 (342)				1 $505	2.5" L 2.25" D
Sensotec	A5	2 (285)	Bonded Strain Gage	20 mV FS	±0.5%	1% per 100°F	1% per 100°F	3 (342)				1 $410	2.5" L 2.25" D
Sensotec	A10	2 (285)	Bonded Strain Gage	30 mV FS	±1%	1.5% per 100°F	2% per 100°F	3 (342)				1 $380	2.5" L 2.25" D
Celesco	P70	±0.1 to ±500	Diaphragm Variable Reluctance	25 mV/V at 3000 Hz	±0.7% of Range	< 1.7% error per 100°F	Thermal			200% of range		1 $251	14 oz
C.J. Enterprises	CJVR	±0.1 to ±500	Diaphragm Variable Reluctance	50 mV/V at 5000 Hz	±0.7% of Range	1.8% error per 100°F	Thermal			200% of range		1 $300	15 oz
Gould Stratham	PL 872 -5	5 (435)	Diaphragm Deposited Strain Gage	30 mV FS	±0.2%	0.5% per 100°F	0.5% per 100°F		±2% FS	200% of range		1 $550	14oz
Bourns	200 - 538 - 1002	(40) to (400)	Diaphragm with Potentio-meter	10 V FS	±2% FS Voltage Ratio	1.5% error per 100°F		Output is linear with airspeed				1-10 $380	13 oz
Schaevitz	PTD - 310 D - 50 W	1.84 (270)	Diaphragm Capsule with LVDT	2.5 V FS	±1.1%	Operating temp. range -65°F to 200°F			Adjust			1-2 $445	18 oz

DIFFERENTIAL PRESSURE TRANSDUCERS (airspeed) * linearity, hysteresis, and repeatability

Manufact'r and Life	Model	Range PSID (knots)	Type	dc Sensitivity	*Static Error PSID	Thermal Bias Shift	Thermal Sens. Shift	Over Range PSID (knots)	Initial zero Balance	Over Pressure		Qty Price	Size or Weight
Sundstrand	314 D	5 (435)	Servo	0 to 10 V FS	±0.057%	0.4% per 100°F	0.5% per 100°F					1 $810	1.6" x 1.6" x 1.9"
Viatran	220		Diaphragm with Strain Gage	High Level Available					Adjust				
Consolidated Controls	41GB67	0 - 0.3 to 0 - 200	Inconel-X Diaphragm with LVDT	High Level									1.4" D 3.9" L
Gulton	GS 614	0 to 5 (435)	Aneroid capsule with LVDT	0 to 5 V ±0.1 V	±1.5%	Thermal sens. ±2% max from -65°F to 225°F				1.25 x range			4 oz
Kulite	SVQH - 500 - 5	5 (435)	Int. ckt silicon diaphragm diffused strain gage	50 mV FS	±0.56%	2% per 100°F	2% per 100°F		±5% FS	4 x range	"		0.6" D 1" L
Daytronic	502	5 (435)	Diaphragm with Strain Gage	30 mV FS	±0.25%	0.5% per 100°F	0.5% per 100°F		±2% FS	1.5 x range		1 $285	2.5" D 3.5" L
Honeywell	HG-280 Data Computer	Air	Silicon Pressure Sensor	General purpose CPU employed			0.1 knot resolution		Sensor separately	not sold	Alt. + Air-speed + Mach	1 $15K	19 lb

DIFFERENTIAL PRESSURE TRANSDUCERS (airspeed) * linearity, hysteresis, and repeatability

Manufact'r and Life	Model	Range PSID (knots)	Type	dc Sensitivity	*Static Error PSID	Thermal Bias Shift	Thermal Sens. Shift	Over Range PSID (knots)	Initial zero Balance	Over Pressure		Qty Price	Size or Weight
Conrac	4715H-D	10 (1400)	Silicon capsule and strain gage	5 V FS	±0.4%	0.5%	0.5%		±1% FS	2 x range		1 $1500 35 $700	
National	LX1501D	-5 to 5 (435)	Solid state silicon	+2.5 V to +12.5 V FS	6% of 5 PSID	6% per 100°F	6% per 100°F		inc. in static error	40 PSID		1 $85	5 gm
Transducer Systems Inc.	ac/ac dc/dc	2.5 (315)	LVDT	100 mV RMS or 2 Vdc FS	±2%	1% per 100°F					-25°F to 300°F op.	1 $150 ac $250 dc	D: ac 1½", dc 2"; L: ac 2", dc 3½"
Robinson-Halpern	150	3 (342)	Capsule + LVDT + electronic circuit	0 to 1 V	±1%	Cal. at 30°F and 150°F within ±2% of 75°F cal.			Factory set ±1% FS	1.5 x range	-40°F to 220°F op.	1 $130	8 oz
Rosemount	1221B3	2.456 (300)	Capsule cap p.o. electronics	6.14 V FS	±0.1% inc. in op. accy.	operating accuracy ±0.5% -55°C to +71°C			Inc. in op. accuracy			1 $785	13 oz
Rosemount	542K2	High level dc outputs	Altitude: / airspeed: / dynamic	h / IAS / pressure:	-1000' / 75 / qc	'To +40,000' / to 340 knots / 0.27 to 6.29" Hg.		±(40' + .7% reading) / ±(2.5K + .4% reading) / ±(.5% FS + 1% reading)		-45°F to +160°F	.2mV/ft / 20mV/K / 1V/"Hg	1-5 $2360 / 12-24 $2125	2 lb

DIFFERENTIAL PRESSURE TRANSDUCERS (airspeed) * linearity, hysteresis, and repeatability

Manufact'r and Life	Model	Range	Type	dc Sensitivity	Non-linearity	Thermal Bias Shift	Thermal Sens. Shift	Actuation Force	* Static Error Band			Qty Price	Size or Weight
Celesco	TCC - PT - 101	Up to 500"	Cable pot spring return	10 V FS	< 0.1%								5¼" x 2" x 2½"
Bourns 40 x 10^6 cycles	194	8"	Linear pot	10 V FS	±0.5%	Temp -65°F	Range to 350°F	1 lb max			Sealed	1 $131 25 $104	0.75" D 11" L
Bourns 40 x 10^6 cycles	163	1,2,3 and 4"	Linear pot	10 V FS	±0.5%	Temp -65°F	Range to 350°F	1 lb max			Sealed	1 $255 25 $135	0.375" D By 3,4,5 or 6"
BLH Electronics 10^6 cycles	416347 416348 416349 423977	.1,.3, .75 and 2"	Resistive	22.5 to 45 mV FS		2% per 100°F	0.5% per 100°F	25 gm	0.25% (0.5% for 2")		+15°F to 115°F op. range	1 $145 .1-.75" $225 2"	8-12 oz
West Coast Research	557	±0.01" to ±10"	Beam deflection with strain gage	3 mV/V to 5 V FS	0.05%	Thermal Sensitivity 0.2% per 100°F							1" cube
West Coast Research	557 L	0 to 0.5" or ±0.25"	same	20 mV FS	0.75%	0.5% per 100°F			2%		-40 to 350°F expo-sure range		1" x 1.5" x 3.5" 3/8" shaft
Alltech	1800	Up to 300"	Cable pot spring return						Up to 0.05%				
Kavlico 50,000 Hrs	Many	±0.05" to 6" stroke	LVDT	400 Hz to 3 kHz 1V/in/V typ.	0.4% typ.		0.1% per 100°F	4 oz typ.		5° phase 30 mV null typ	-420°F to +450°F typ.op.		Many

LINEAR DISPLACEMENT TRANSDUCERS

* nonlinearity, hysteresis, nonrepeatability

Manufact'r and Life	Model	Range	Type	dc Sensitivity	Non-linearity	Thermal Bias Shift	Thermal Sens. Shift	Actuation Force	*Static Error Band			Qty Price	Size or Weight
Humphrey 10^6 cycles	RP93-0101-1	0.25" to 1" stroke	Linear pot	10 V FS	1%					0.0014" resolution	Larger models available		0.24 oz
The Accro Co.	Series 1850	2" to 180"	cable pot spring return	0.044 to 460mV/in	±0.1%			18 to 48 oz		4 g cable accel	-65°F to 160°F op.		1"x5"x3" for 2" range
Temposonic	DCT-12 --- DCT-60	12" to 60"	Ultrasonic Magnetic	10 V FS or digital	0.1%		1% per 100°F	Non-contesting	0.11%		35°F to 125° op.	From $295 to $700	4" x 5.5" x 2.5"
Honeywell	SB 80 and SB 82	±0.25" to ±1"	LVDT	AC 1.6 to 4.6 mV/V DC 0.4 mV/V	0.5 to 0.7%			2.5 or 6.5 lb per in.		Sealed shaft	-40 to 135°F op.		1.2 to 2" 10 to 16"
Hewlett Packard	Series 7DCDT and 24DCDT	±0.05" to ±3"	LVDT	4.3 to 100 V/in	±0.5%			Non-contacting free slug				1 $130 to $270	23 to 220 gm
Moxon	1104 1105 1110 1111	±0.05" to ±3"	LVDT	±0.4 V or ±10 V FS	±0.25% or ±0.1%	1 or 2% per 100°F		optional spring 2.5 oz/in	±0.25% or ±0.1%			1 $145 to $240	0.75" D 3 to 14" Length
Transducer Systems Inc.	L1000 L2000 L3000 L6000	±1" to ±6" others down to ±0.005"	LVDT	AC 0.2 to 0.7 mV/V/mill	1 to 2% others 0.1%			Non-contacting free slug				1 $125 $175 $235 $375	5/8 to 7/8" D 4.5 to 25" length

LINEAR DISPLACEMENT TRANSDUCERS

* nonlinearity, hysteresis, nonrepeatability

Manufacturer and Life	Model	Range	Type	dc Sensitivity	Nonlinearity	Thermal Bias Shift	Thermal Sens. Shift	Actuation Force	*Static Error Band			Qty Price	Size or Weight
Schaevitz	Many	±0.05 " to ±10"	LVDT	ac 0.1 to 6mv/V per mil	0.05% to 4%			Non contacting free slug			-65°F to 300°F op.	1 $32 to 430 6-11 $28 to 387	4 to 580 gm 1 to 30 inches
Robinson Halpern	220 Series	±0.005" to ±18"	LVDT	ac 0.7 to 10 mV/V/mil	±0.07% to ±0.5%	0.3% to 10% per 100°F		Non contacting free slug		60 Hz to 20 kHz units			3/8 or 7/8" D 0.5 to 18" L
Aviation Electric Ltd.	1303 1343 1353 1315 1362	1.27mm 2.5 10 25.4 76.2	LVDT	±5 V ±10 V ±5 V " ±3 V	±0.15% to ±1%			Spring loaded or free slug or self-aligning bearing		Linear pots also available 12.5 to 2540 mm stroke			

LINEAR DISPLACEMENT TRANSDUCERS

* nonlinearity, hysteresis, nonrepeatability

APPENDIX B

ADDITIONAL ANGULAR ACCELERATION DISCUSSION (Ch. 4)

The angular accelerometers available measure the torque to accelerate an inertia of rigid or liquid matter. In principle, linear accelerometers can be used differentially. If only two are used, they are sensitive to an angular velocity vector component in the plane of their separation and sensitive axes. A set of four at right angles can be used to cancel this effect, or three can be deployed in a plane with the input axes 120 degrees apart.

The measurements for two units as shown in Fig. B-1 are

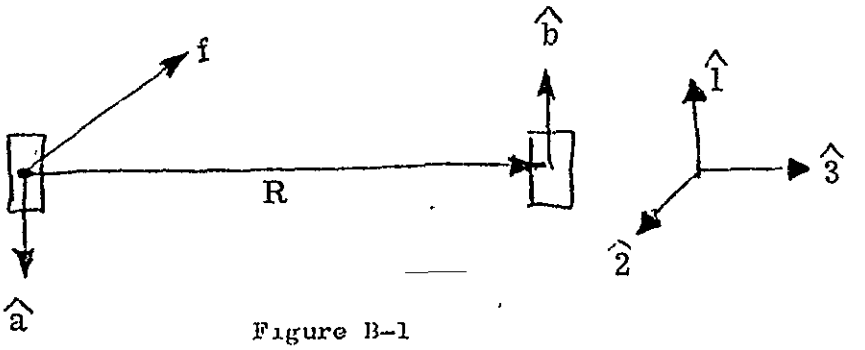

Figure B-1

$$y^a = \{f \cdot \hat{a}\} K_a$$

$$y^b = \{f \cdot \hat{b} + [(\dot{\omega} \times R + \omega \times (\omega \times R)] \cdot \hat{b}\} K_b$$

For the ideal case with $\hat{a}$ and $\hat{b}$ parallel and each perpendicular to R and $K_a \equiv K_b = 1$.

$$y^a + y^b = R\alpha_2 + R\omega_1\omega_3 .$$

Thus the signal that is the sum of the accelerometer outputs measures angular acceleration but has error terms proportional to the products of

the two angular velocities. If four are used as shown in Fig. B-2, there is no error.

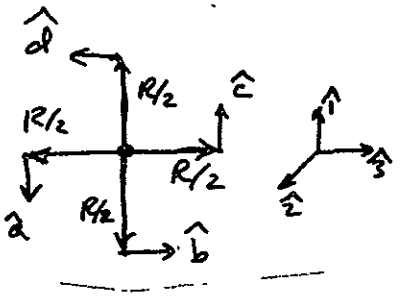

$$y^a + y^b + y^c + y^d = 2R\alpha_2 + R[\omega_1\omega_3 + (-\omega_3)\omega_1]$$
$$= 2R\alpha_2 .$$

Fig. B-2

Similarly, for three units in a plane as shown in Fig. B-3

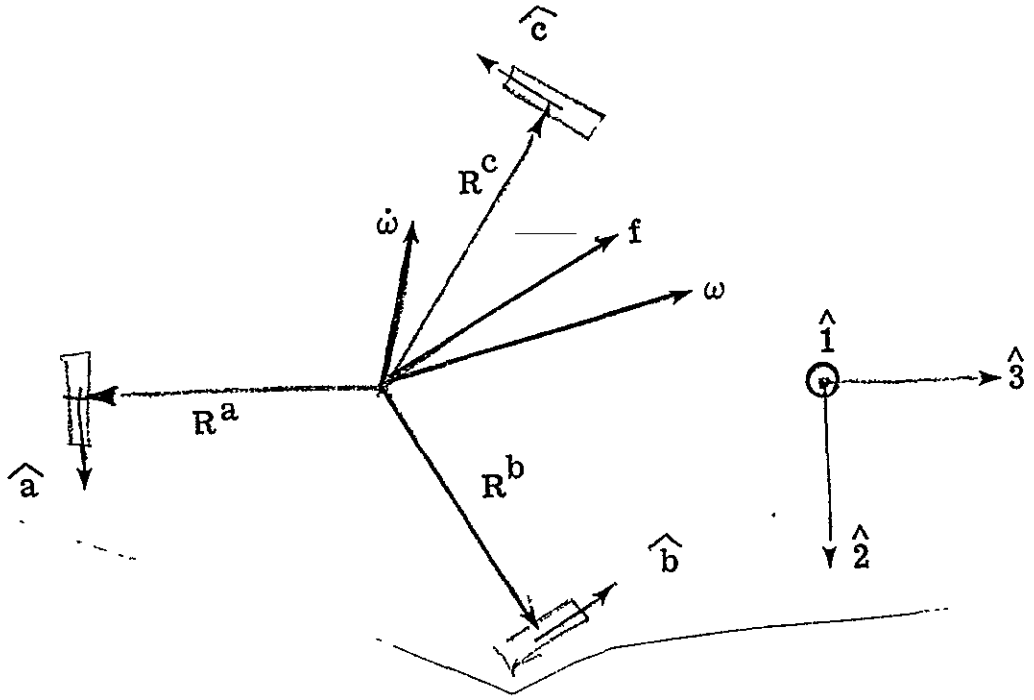

Figure B-3

with

$$\hat{a} = \begin{bmatrix} 0 \\ 1 \\ 0 \end{bmatrix}, \quad \hat{b} = \begin{bmatrix} 0 \\ -0.5 \\ 0.86 \end{bmatrix} \quad \hat{c} = \begin{bmatrix} 0 \\ -0.5 \\ -0.86 \end{bmatrix} \quad R^a = \begin{bmatrix} 0 \\ 0 \\ -R \end{bmatrix} \quad R^b = \begin{bmatrix} 0 \\ 0.86R \\ 0.5R \end{bmatrix}$$

$$R^c = \begin{bmatrix} 0 \\ -0.86R \\ 0.5R \end{bmatrix}$$

each measurement is of the form

$$y^a = (f + \omega \times R^a + \omega \times \omega \times R^a) \cdot a .$$

This configuration rejects the effect of linear specific force as before.

Thus, three, four or more accelerometers can be located in a plane in a configuration that is insensitive, in principle, to angular velocity, but two accelerometers are not adequate due to their intrinsic sensitivity to angular velocity.

Accuracy Requirements for Angular Accelerometers

For 10 millirad angle information accuracy, the angular accelerometer performance requirement depends upon the amount of time that errors are permitted to grow. Rapid roll angular determination with a rolling mode time constant of a few 10ths of a second would correspond to perhaps 1 sec smoothing time, whereas spiral and phugoid modes may require 100 times as long, thus the minimum error or undetected rate would be from 2×10^{-2} to 2×10^{-6} rad/sec^2. Assuming a maximum rolling rate of about 180 deg/sec and a rolling mode time constant of 0.1 sec, the maximum angular acceleration would be approximately 30 rad/sec^2. We can calculate a dynamic range for the instrument as 0.01 to 10 rad/sec^2 for an absolute minimum, 0.4×10^{-3} to 30 rad/sec^2 would be more desirable, and 10^{-6} to 100 would give more information than is needed. Assuming a 10 cm separation between accelerometers, the equivalent linear acceleration uncertainty for even the minimum range is 10^{-4}g and this may be below the level of some accelerometers that would be acceptable for measuring the linear

In addition to basic sensitivity, the alignment, scale factor matching, and linearity must be in the 10^{-6} range to reject the 1 g specific force.

Angular accelerometers, therefore, should be special purpose devices rather than a set of linear accelerometers for the aircraft autopilot measurement application.

REFERENCES

1. DeBra, D.B., and A.E. Bryson, "Minimum Cost Autopilots for Light Aircraft," Invited Paper presented at the VI IFAC Symposium on Automatic Control in Space, 26-31 Aug. 1974, Tsakhkadzor, Armenian SSR, USSR.

2. Breza, M.J., and A.E. Bryson, "Minimum Variance Steady State Filters with Eigenvalue Constraints," Dept. Aeronautics and Astronautics, Stanford University, Stanford, Calif., To be published.

3. Pietila, R., and W.R. Dunn, "A Vector Autopilot System," IEEE Trans. on Aerospace and Electronic Systems, Vol. AES-12, No. 3, May 1976.

4. Iliff, K.W., and M.F. Shafer, "Flight-Determined Stability and Control Characteristics for a Light Twin-Engined General Aviation Airplane," to be published as a NASA TN, The NASA, Washington, D.C., 1976 (Feb).

5. Wolowicz, C.H., and R.B. Yancey, Longitudinal Aerodynamic Characteristics of Light, Twin-Engine, Propeller-Driven Airplanes," NASA TN-D-6800, The NASA, Washington, D.C., Jun, 1972.

6. Blakelock, H.H., Automatic Control of Aircraft and Missiles, Wiley, New York, 1965.

7. Sorensen, J.A., "Analysis of Instrument Error Effects on the Identification Accuracy of Aircraft Parameters," NASA CR-112121, The NASA, Washington, D.C., May 1972.

8. Sorensen, J.A., "Application of State Estimation Techniques for Development of Low Cost Flight Control Systems," to be published as a NASA TMX, The NASA, Washington, D.C., 1976.

9. Final Report on "Study to Determine the Applicability of Integrated Circuit Sensor Technology to General Aviation Orientation Estimation," submitted to NASA Ames Research Center by Stanford University, Guidance & Control Laboratory, Dept. Aeronautics and Astronautics, Stanford, Ca., 94305, Sept. 1976.